LLOYD'S

Emerging Risk Report – November 2016

NATURAL ENVIRONMENT

The risk of global weather connections

Are atmospheric hazards independent?

Met Office

Disclaimer

This report has been produced for Lloyd's by the Met Office for general information purposes only. While care has been taken in gathering the data and preparing the report, Lloyd's does not make any representations or warranties as to its accuracy or completeness, and expressly excludes to the maximum extent permitted by law all those that might otherwise be implied.

Lloyd's accepts no responsibility or liability for any loss or damage of any nature occasioned to any person as a result of acting or refraining from acting as a result of, or in reliance on, any model, statement, fact, figure or expression of opinion or belief (or any part thereof) contained in this report. This report does not constitute advice of any kind.

The Met Office aims to ensure that the content of this document is accurate and consistent with its best current scientific understanding. However, the science which underlies meteorological forecasts and climate projections is constantly evolving. Therefore, any element of the content of this document which involves a forecast or a prediction should be regarded as the Met Office best possible guidance, but should not be relied upon as if it were a statement of fact. To the fullest extent permitted by applicable law, the Met Office excludes all warranties or representations (express or implied) in respect of the content of this document.

Use of the content of this document is entirely at the reader's own risk. The Met Office makes no warranty, representation or guarantees that the content of this document is error-free or fit for your intended use.

Before taking action based on the content of this document, the reader should evaluate it thoroughly in the context of his/her specific requirements and intended applications.

To the fullest extent permitted by applicable law, the Met Office, its employees, contractors or subcontractors, hereby disclaim any and all liability for loss, injury or damage (direct, indirect, consequential, incidental or special) arising out of or in connection with the use of the content of this document including without limitation any and all liability:

- Relating to the accuracy, completeness, reliability, availability, suitability, quality, ownership, non-infringement, operation, merchantability and fitness for purpose of the content of this document
- Relating to its work procuring, compiling, interpreting, editing, reporting and publishing the content of this document
- Resulting from reliance upon, operation of, use of or actions or decisions made on the basis of, any facts, opinions, ideas, instructions, methods, or procedures set out in this document

Nothing in this disclaimer affects the Met Office's liability for death or personal injury arising from the Met Office's negligence, or the Met Office's liability for fraud or fraudulent misrepresentation, or any other liability which cannot be excluded or limited under applicable law.

If any of these provisions or part provisions are for any reason held to be unenforceable, illegal or invalid, that unenforceability, illegality or invalidity will not affect any other provisions or part provisions which will continue in full force and effect.

Key Contacts

Trevor Maynard
Head, Exposure Management and Reinsurance
trevor.maynard@lloyds.com

Lucy Stanbrough
Executive, Emerging Risks and Research
lucy.stanbrough@lloyds.com

For general enquiries about this report and Lloyd's work on emerging risks, please contact emergingrisks@lloyds.com

About the authors

Hamish Steptoe is an applied climate scientist with the insurance and capital markets team at the Met Office. He holds an MSc in applied meteorology from the University of Reading and a second MSc in earth science from Utrecht University, The Netherlands. Since starting at the Met Office in 2014, Hamish has been involved in developing products for European windstorms, whilst continuing research into the representation of large-scale climate process in global climate models at the University of Reading. He has also been involved in projects for the BBC and the Royal Meteorological Society and has advised on the scientific aspects of recent expeditions to Madagascar, Mongolia and the Indian Himalayas.

Trevor Maynard PhD, MSc, FIA has degrees in pure maths and statistics and is a Fellow of the Institute of Actuaries. He is head of exposure management and reinsurance at Lloyd's and is responsible for monitoring the natural and manmade aggregations of risk across the Lloyd's market including emerging risks. Subjects covered in recent years include: the economic and social implications of a food system shock; the effects of cyber-attacks on the US energy grid and an exploration of aggregation modelling methods for liability risks.

He is co-chairman of OASIS, an open modelling platform for catastrophe models and sits on the Board of the Lighthill Risk Network.

Acknowledgements

Lloyd's would like to thank the following people for their contribution in reviewing various aspects of this study: Mike Davey from the Centre for Science and Policy, University of Cambridge; Theo Economou, Helen Fox, Emily Wallace, Paul Maisey, Ed Pope, Chris Kent, Jennifer Rourke and Steven Wade from the Met Office .

Lloyd's is also grateful to Ed Wheatcroft from the Centre for the Analysis of Time Series at the London School of Economics for carrying out a statistical study of past extreme events in the region-perils specified. His work augments the driver-based study that occupies the majority of this paper.

Lloyd's 'The risk of global weather connections' project team:

Trevor Maynard, Exposure Management and Reinsurance

Sundeep Chahal, Lloyd's Catastrophe Model

Lucy Stanbrough, Emerging Risks and Research

Contents

Executive summary

Background

Major atmospheric-driven catastrophes, such as hurricanes and floods, may appear to be independent events when looked at historically. Yet it is well established in climate science that regional weather and climate conditions in one part of the world can have impacts on other parts. Changes in temperature or humidity that result in increased rainfall in one ocean basin might also create conditions favourable for storm development that affect communities thousands of kilometres away.

In weather and climate science, links between extreme weather events occurring in separate regions of the world, taking place over timescales from days to years, are known as teleconnections.[1]

The best known teleconnection, the El Niño Southern Oscillation phenomenon, drives changes in weather patterns globally by affecting large-scale atmospheric circulation across the tropics. These changes modify rainfall patterns and can cause flooding, droughts and heatwaves.[2] El Niño years typically have more active Pacific typhoon seasons while La Niña years, the opposite phase, represented by colder than normal sea surface temperatures, typically have more active Atlantic hurricane seasons. Given the interconnected nature of the "Earth system" – the Earth´s interacting physical, chemical, and biological processes – it is therefore possible for weather events or perils in different regions (known as region-perils) to be connected to the same driver.

Implications of weather connections for insurers

But just how interconnected are these climate drivers? The answer to this question is important for insurers, and particularly reinsurers, both of whom are required by regulators to hold a level of capital that adequately reflects their exposure to losses from significant weather events. It is the insurer's responsibility to demonstrate to the regulator that they hold adequate levels of capital. For example, the Corporation of Lloyd's uses an internal model to calculate the capital required by the market, this model covers many perils, such as hurricane risk, windstorms, winter storms, hail and flooding, in multiple regions around the world to show that its capital is adequate.

The Corporation of Lloyd's internal model is based predominantly on the assumption that extreme weather events occur independently of each other. Recently, however, some in the regulatory community have started to question whether extreme weather events are more interconnected than previously thought and whether the assumption of independence is appropriate. If it is not, regulators could require insurers and reinsurers to hold more capital to cover their exposure to potentially greater insurance losses. This requirement would tie up funds that could otherwise be allocated to new business development, such as developing products for new threats e.g. cyber risks.

To establish whether the assumption of independence in insurers' internal models is appropriate, and to increase insurers' and regulators' understanding of the implications of teleconnections for risk modelling, Lloyd's commissioned the Met Office to investigate the extent of the links between different global extreme weather perils and the mechanisms for these dependencies.

This report answers the question: is it reasonable to assume independence between significant weather risks in certain region-perils around the world?

Groundbreaking methodology

Lloyd's worked with the Met Office to develop an innovative methodology for assessing the interconnectivity of global weather events. The comprehensive approach detailed in this study is believed to be unique because it analyses the potential links between weather events globally, whereas existing methodologies cover single regions only.

And in a groundbreaking move, Lloyd's and the Met Office have disclosed the methodology in full for general review purposes and to encourage debate (*see Appendix A for full details of the methodology*). Both Lloyd's and the Met Office hope that by adopting this approach other modellers can add to and improve the methodology.

To create the methodology, 16 region-perils were chosen on the basis of their relevance to the Lloyd's market. The Met Office then identified 22 potential "Earth system drivers" (such as El Niño) that could be connected to these region-perils. The Met Office selected nine of these based on characteristics of influence and seasonality that related most closely to answering the question of independence posed by Lloyd's.

The next stage involved analysing the various interactions between perils and climate drivers, which showed the extent of the potential connections between weather events. The degree of correlation between the climate drivers and the chosen region-perils was then assessed following a comprehensive review of existing research literature from more than 200 sources (*see Appendix C*). Last, a model was run to produce 16 region-peril indices which captured the background level of risk for each peril.

From this data the Corporation of Lloyd's was able to assess whether the assumption of independence between weather events is appropriate.

Additional research

To complement the main approach in this paper Lloyd's also worked with Ed Wheatcroft, an independent statistics consultant based at the Centre for Analysis of Time Series, London School of Economics

His data-driven statistical study (*see Section 3.1, Box 2, p30*) considered the assumption of independence from a number of different angles, including whether it is reasonable to assume so between perils of the same type, whether there are links between different types of perils and whether there is evidence to reject the assumption of independence when considering significant weather events that take place simultaneously. The study looked at whether there was any significance in the number of times each type of peril took place annually using available data sources.

This conclusion of this second study is consistent with the findings set out below.

The key findings

1 **For extreme weather events an assumption of independence is appropriate.**
The results of running the methodology in this report through the Corporation of Lloyd's internal model demonstrate that the assumption of independence between weather events in models used by the insurance industry remains appropriate.

2 **A number of regions show some correlation between climate drivers but these are not considered to be substantial enough to warrant a change in our capital.**
While there is some level of dependency between perils, the findings of both the data-driven statistical study (*see Section 3.1, Box 2, p30*) and the model presented in the main body of this study are that the impact of this on insurance capital modelling is negligible. Only nine of the 120 peril correlations analysed in this study showed any significant links, and the links can be both positive and negative. For example, the study confirmed that while the El Niño-Southern Oscillation influences the majority (14 of 16) of regional weather perils, it also reduces the impact of 10 of the 14 perils for three months of the year.

3 **Even when there are high correlation levels between weather events, it does not necessarily follow that there will be large insurance losses.**
For atmospheric hazards to cause major insurance losses, a rare major atmospheric event has to take place in combination with other circumstances conducive to such losses (e.g. a weather event affecting a major urban centre). Such circumstances are so rare that even when atmospheric conditions are conducive to a major weather event, they do not always occur. Conversely, large losses sometimes occur in years when the correlation levels are not as high. For example, Hurricane Andrew (*see case study, p6 and p33*), which caused one of the largest insurance losses of the 20th century, occurred in an El Niño year – a climatic feature that tends to reduce the likelihood of hurricane development.

4 **Weather events can still occur simultaneously even if there is no link between them.**
Extreme weather events can still take place at the same time even though this study confirms that weather events can be modelled as independent. Indeed, the Corporation of Lloyd's internal model generates scenarios that show multiple massive catastrophes occurring in the same year, despite underlying assumptions of independence.

Overall conclusion

The results of the modelling presented in this study demonstrate that an assumption of region-peril independence is currently appropriate for use in modelling extreme natural catastrophe risks.

This important finding supports the broader argument that the global reinsurance industry's practice of pooling risks in multiple regions is capital efficient and that modelling appropriate region perils as independent is reasonable.

This challenges the increasingly held view among some regulators around the world that capital for local risks should be held in their own jurisdictions. Lloyd's believes this approach reduces the capital efficiency of the (re)insurance market by ignoring the diversification benefits provided by writing different risks in different locations and, in so doing, needlessly increases costs, to the ultimate detriment of policyholders. Insisting on the fragmentation of capital is not in the best interests of policyholders.

Next steps

Modellers can use external data creatively and innovatively to complement the insurance market's specialist data, and both Lloyd's and the Met Office have disclosed the methodology in full for general review purposes to encourage debate (*see Appendix A for full details of the methodology*). Lloyd's welcomes dialogue and development from any and all sectors to add to and improve the methodology.

Whilst future studies could use numerical weather predication models to further assess these implications (*see p36 for more details*), Lloyd's believes that additional modelling efforts would be best directed to further studies. These could focus on topics such as augmenting the list of historical events with simulated examples to ensure that insurers are prepared for the full range of potential risks.

Note on the methodology

While this report finds that an assumption of independence is appropriate when modelling weather-related insurance losses, it is important to recognise the limitations of the methodology presented, which is based on the current state of climate dynamics and does not account for possible future change in the Earth's climate system. It is also based on assumptions that any interaction between weather events is captured by the methodology's driver simulations.

Case study – Hurricane Andrew

This case study highlights the potential for extreme events to occur even though climate conditions are unfavourable for their development.

Hurricane Andrew is a good illustration of this. Andrew made landfall as a Category 5 hurricane in August 1992 in Miami, Florida. Described by the Miami Herald at the time as "the worst natural disaster ever to befall the United States", it destroyed 63,000 homes, left up to 250,000 people homeless and, according to the National Hurricane Center, led directly to 26 deaths and contributed to 39 more.[3]

And yet the 1992 hurricane season as a whole was not very active, in line with the characteristics of the El Niño phase. One measure of hurricane season strength is known as the Accumulated Cyclone Energy (ACE) Index. In 1992, the ACE Index was below normal at 76, compared to 250 in 2005, the highest ever recorded.[4] In other words, climatic conditions were not conducive to a hurricane but Andrew took place anyway.

In terms of its impact on the insurance industry, despite being a relatively small storm, Andrew's landfall on 24 August caused US$25 billion-worth of economic damage, $15 billion of which was insured[5] ($27 billion in today's terms[6]).

1 Introduction

This study considers climate drivers – those local or regional modes of the atmosphere-ocean system that have a significant impact on large-scale weather patterns – and teleconnections – the remote influences that these drivers have on weather patterns. Many studies in academic literature focus on the connection between a specific climate driver and a chosen peril in a particular region, such as the wetter-than-average rainfall tendency during August-November over the Iberian Peninsula due to El Niño. Studies of the likely interactions between climate drivers and perils on a global scale are more limited in number.

This interaction between climate drivers and perils on a global scale is important to explore because any material levels of dependency between the major atmospheric risks covered by insurance could require an increase in the level of statutory capital held by the insurance industry.

An in-depth review of available literature relating to the nine key climate drivers and 16 region-perils that were determined to be of interest, was used alongside statistical analysis to explore the question. The result is a matrix of correlations along with a global map to illustrate connections (*see Section 3, p24*).

The Met Office approach to address the peril interdependency was to consider which key drivers of the global climate (such as El Niño-Southern Oscillation) are important for a specified list of perils, representing key areas of insurance exposure for the Lloyd's market.

The Met Office developed a model that takes simulated driver information and uses these to produce a "peril index" for each peril. Positive values of the index indicate a higher tendency of occurrence for that peril in the year and negative values indicate a lower tendency of occurrence. The final step in the modelling process was to link the peril indices to modelled extreme events and insurance losses. The model demonstrates that multiple drivers can often affect a single region-peril and that the dependency between the region-perils typically arises from shared drivers.

2 Methodology

Figure 1 (*see p9*) illustrates the processes followed in this project; the layout of the following sections matches these steps.

In summary, the approach taken in this study is as follows:

Climate drivers and teleconnections: In this study Lloyd's considers climate drivers – those local or regional modes of the atmosphere-ocean system that have a significant impact on large-scale weather patterns – and teleconnections – the remote influences that these drivers have on weather patterns. Many studies in literature focus on the connection between a specific climate driver and a chosen peril in a particular region, such as the wetter than average rainfall tendency during August-November over the Iberian Peninsula due to El Niño, but work looking more widely at the likely interactions between climate drivers and perils on a global scale is more limited. This is a very complex picture and something that is addressed in this study with reference to currently available literature and statistical analysis.

Selection of region-perils and drivers: First key region perils were specified (*Section 2.1*), then potential drivers were identified that might influence these region perils (*Section 2.2*). Relevant climate drivers were associated with an initial list of perils and regions proposed by Lloyd's. This selection was reduced to a list of nine key climate drivers (*see Section 2.3*) that were assessed as being mechanistically sufficiently distinct, demonstrating a suitably robust relationship with region-perils and occurring on a timescale commensurate with the annual decision-making cycle of the reinsurance industry. These drivers were also sufficiently well covered in the literature to allow analysis of dependency to be made with some level of confidence. To represent lagged and non-lagged interactions of seasonal climate drivers, the auto-correlation of each driver and the cross-correlation between driver pairs was modelled.

Correlation of drivers and region-perils using literature: From a review of articles in the academic literature relating to the nine key climate drivers and 16 region-perils, an assessment was made of the correlation coefficient for each peril-driver interaction. (*see Appendix section C for a selected bibliography of material reviewed*). The approach sought to maximise the use and value of the available information: where multiple correlation values were available, these were appropriately averaged; where evidence is provided but no correlation value given then an estimate is made; where a strong relationship has been identified based on compelling evidence or supported by multiple sources of evidence this has been highlighted. This analysis was then further subjected to peer review by subject matter experts to ensure that the analysis could plausibly be defended.

Statistical modelling of peril-driver interactions: The interconnected nature of the Earth's climate system meant that it was necessary, at the next stage, to model not only the interactions of two perils with one climate driver, but also the interactions of a set of perils with two or more drivers, to represent the case where drivers have an modulating effect on each other as well as on the region-peril under analysis. The result is a matrix of correlations (*illustrated in Section 3, p24*) for the full set of perils identified at the outset of the study.

Monthly index data for the nine drivers, taken from between 1979 and 2015, then formed the basis of a coupled statistical model capturing the dependency structure between the drivers, described in Section 2.4 (*and in full in Appendix section A2*). This enabled a further statistical modelling of the region-peril index behaviour as a function of the drivers to be developed, as described in Section 2.5. Peril indices describe the level of background risk in a given year for a certain region-perils – a high peril index does not necessarily lead to an extreme event in that year since these are random and depend on multiple features. The process for modelling extreme events given a certain peril index is then described in Section 3.1.

Key peril-peril correlations and limiting factors: Only nine of 120 peril-peril correlations are significantly different to zero at 90% confidence (meaning that the correlations are unlikely to have occurred by chance, not that they are of particular importance), based on currently available evidence (which does not mean that the others do not exist and may not be found to be more significant in future, either through further research or as a result of the impacts of climate change). El Niño-Southern Oscillation is confirmed as the global driver that influences the majority (14 of 16) of regional perils investigated in this study. For 10 of the 14 perils it is a significant source of peril modulation for more than three months of a year.

Conditional event sampling: The model presented here creates an index for each chosen region-peril. A high level of the index indicates an increased background risk for the peril. This does not imply that an extreme financial event will arise – it simply makes it more likely. The most extreme financial events typically require a whole chain of unlikely things to occur. Some of these are captured by the index (such as a hurricane forming and being stronger than average) but others (such as the fact the hurricane is a high category that makes landfall hitting a particular city at high tide) are not captured by the index. This residual randomness is captured within the model by further Monte Carlo sampling from a loss distribution that has been adjusted by the index. Lloyd's calls this conditional event sampling. Even without this step the study found that the low levels of correlation in the

Figure 1: Project process flow chart

Source: Lloyd's.

region-peril indices do not materially challenge Lloyd's assumption of independence.

Limitations: In some instances evidence of a correlation is contradictory, limiting the strength of any conclusions on the relationship. Not all studies compare the same regions (a sub region of a country for example) and not all studies investigate correlations with the same meteorological attributes (e.g. flooding vs rainfall rate), leading to further uncertainties in the evidence. It is important to note that some oscillation between positive and negative phases of some drivers are thought to be non-stationary over long time periods, which is something that is not accounted for in this work. Similarly, the effect of large scale global climatic change is not incorporated. Lloyd's also assumes that any driver-driver interaction in either the form of driver-to-driver enhancement or diminishment is captured by the study's tiered driver simulations. In areas where the evidence is contradictory or limited, targeted further research would enable more robust evidence to be generated and may alter some of the conclusions of this study.

Methodology summary

First key region perils were specified (*Section 2.1*), then potential drivers were identified that might influence these region perils (*section 2.2*). These were rationalised to nine key drivers based on criteria described in Section 2.3. From a review of articles in the academic literature relating to the nine key climate drivers and 16 region-perils, an assessment was made of the correlation coefficient for each peril-driver interaction (*see Appendix section C for a selected bibliography of material reviewed*).

The approach sought to maximise the use and value of the available information: where multiple correlation values were available, these were appropriately averaged; where evidence is provided but no correlation value given then an estimate is made; where a strong relationship has been identified based on compelling evidence or supported by multiple sources of evidence this has been highlighted. This analysis was then further subjected to peer-review by subject matter experts to ensure that the analysis could plausibly be defended.

Monthly index data for the nine drivers, taken from between 1979 and 2015, then formed the basis of a coupled statistical model capturing the dependency structure between the drivers, described in Section 2.4 (*and in full in Appendix section A2*). This enabled a further statistical modelling of the region-peril index behaviour as a function of the drivers to be developed, as described in Section 2.5. Peril indices describe the level of background risk in a given year for a certain region-peril – a high peril index does not necessarily lead to an extreme event in that year since these are random and depend on multiple features. The process for modelling extreme events given a certain peril index is then described in Section 3.1.

The interconnected nature of the Earth's climate system means that it is necessary to model not only the interactions of two perils with one climate driver, but also the interactions of a set of perils with two or more drivers, to represent the case where drivers have a modulating effect on each other as well as on the region-peril under analysis. The result is a matrix of correlations illustrated in Section 3 for the full set of perils identified at the outset of the study, along with further expansion of

Table 1: List of chosen region/perils

Region	Peril
Australia	Flood
Australia	Windstorm
Australia	Wildfire
Brazil	Flood
China	Flood
Europe	Flood
Europe	Windstorm
Gulf of Mexico & Florida	Tropical cyclone
Indian Ocean	Tropical cyclone
Mexico	Flood
North East US & Canada (East Coast)	Tropical cyclone
North West Pacific	Tropical cyclone
South Africa	Flood
Thailand / Malaysia	Flood
US	Flood
US	Tornadoes

the conclusions of the work in Section 4. Finally, future model development ideas are discussed in Section 5.

2.1 Region-peril definition

The following list of regions and perils were chosen for investigation based on key countries and territories of interest to Lloyd's.

2.2 Global climate drivers

Twenty two global climate drivers (*see Table 2, below*) were investigated as part of this process, and in order to further understand the complex interconnected systems that make up the global climate, descriptions of all the drivers considered have been included. This considers other factors such as Arctic sea ice, volcanic eruptions and planetary waves that also act as drivers in the global climate system.

It is important to keep in mind that these drivers operate over a range of temporal and spatial scales – every driver is a cog in a larger machine, and they turn at different speeds with varying levels of impact, some local, some global. Some drivers are thought to be non-stationary – i.e. the timescale over which they operate varies (*see Table 2 below*), and that climatic change can introduce long period changes to driver variability. Both these factors introduce limitations to this work, which are discussed further in Section 3 (*see p28*).

Table 2: Climate driver timescales

Driver	Months	Year	Years	Decadel (<30 years)	Multidecadel (≥30 years)
African Easterly Waves	■				
Antarctic Oscillation/Southern Annular Mode (AAO/SAM)	■	■			
Atlantic Meridional Mode (AMM)	■	■	■		
Atlantic Multi-decadal Oscillation (AMO)					■
Arctic Oscillation (AO)	■	■	■		
Arctic Sea Ice	■	■			
Australian Blocking Index (BI)	■				
Boreal Summer Intraseasonal Oscillation (BSISO)	■				
East Atlantic Pattern(EAP)			■		
El Niño-Southern Oscillation (ENSO)			■		
Indian Ocean Dipole pattern (IOD)					
Inter-decadal Pacific Oscillation (IPO)				■	■
Madden-Julian Oscillation (MJO)	■				
North Atlantic Oscillation (NAO)	■	■	■	■	■
North Pacific Oscillation (NPO)					■
Pacific Decadal Oscillation (PDO)				■	■
Pacific North America pattern (PNA)			■		
Quasi-Biennial Oscillation (QBO)			■		
Rossby Waves (and other planetary waves)	■		■		
Scandinavian Pattern (SCP)					
Southern Oscillation Index (SOI)			■		
Volcanic Eruptions	■	■			

2.2.1 Descriptions of climate drivers

Further source reference materials can be found in Appendix Section C. This will be of interest to anyone looking to gain a greater understanding of the drivers of weather-based perils in regions of interest.

2.2.1.1 African Easterly Waves

African Easterly Waves form in the African Sahel, and are generated by disturbances in the African jet causing kinks in what would otherwise be a constant jet.[7] The jet is created by the strong temperature difference between the Sahara Desert and the Gulf of Guinea. As air warmed over the Sahara rises and turns southward towards the cooler air over the Gulf, the rotation of the Earth turns the air current westwards and this stream continues to flow out over the Atlantic Ocean.[8]

African Easterly Waves propagate westward across the tropical and subtropical North Atlantic and can reach the Caribbean Sea and western North Atlantic, developing into thunderstorms that may then turn into hurricanes with moist air.[9] They have a period of three to four days, a horizontal wavelength of 2,000-2,500km, and maximum amplitude in the lower troposphere. Approximately 60 African easterly waves form between May and October when conditions for the African jet are favourable[10].

2.2.1.2 Antarctic Oscillation/Southern Annular Mode (AAO/SAM)

The Antarctic Oscillation is the change in atmospheric pressure that occurs roughly every month between the Antarctic and southern-middle latitude that brings changes in wind and storm activity.[11] It can be viewed as the south version of the Northern Annular Mode, and appears as two opposite pressure anomalies, one centred over the Antarctic and the other occurring between 40-50°s.[12] It is these changes that cause the north-south movement of the westerly winds that circle the South Pole, with positive phases contracting the belt of winds towards Antarctica that results in a warming of the southern hemisphere mid-latitudes, with the negative phase pushing them further out.[13]

2.2.1.3 Atlantic Meridional Mode (AMM)

The Atlantic Meridional Mode is the dominant source of linked ocean-atmosphere variability in the Atlantic that affects rainfall in northeast Brazil and tropical cyclone development in the North Atlantic[14]. It is characterised by variations in sea-surface temperatures and sea level pressure between the tropical Atlantic north and south of the Intertropical Convergence Zone[15]. It is this interaction in heat exchange between the ocean and atmosphere that drives change. It is also influenced by other drivers, particularly El Niño-Southern Oscillation and North Atlantic Oscillation, and should be considered a distinct mode from Atlantic Multi-decadal Oscillation when looking at short time variations.[16]

During a positive phase, sea surface temperatures become warmer than normal in the tropical North Atlantic and cooler in the tropical South Atlantic. The surface air pressure responds to the changes with lower pressure in the North and higher in the South[17]. These changes in pressure cause the Atlantic Intertropical Convergence Zone – where trade winds come together, triggering storm systems – to be pushed northwards, resulting in drought in northeast Brazil as this mixing zone shifts. Warmer than normal sea-surface temperatures during this cycle also tend to result in more tropical storms developing in the Atlantic. When the Atlantic Meridional Mode is in a negative phase the opposite occurs – greater rainfall in Brazil, and fewer tropical storms in the Atlantic[18].

2.2.1.4 Atlantic Multi-decadal Oscillation (AMO)

The Atlantic Multi-decadal Oscillation is a global mode of natural variability typically reflected in global sea surface temperatures in the North Atlantic Ocean, with cool and warm phases that may last for 20-40 years at a time[19]. It is thought that the changes are driven by fluctuations in the overturning circulation of the Atlantic Ocean, with changes in the sea-surface temperatures influencing air temperatures. These in turn give rise to changes in rainfall over much of the Northern Hemisphere, in particular, North America and Europe[20].

Atlantic Multi-decadal Oscillation has been associated with multi-decadal variations in Indian, East Asian and West African monsoons, the North African Sahel and northeast Brazil rainfall. Warm phases have seen an increase in the frequency and intensity of droughts in the US Midwest and Southwest, and more rainfall in the Pacific Northwest and Florida[21]. Tropical storms are also more likely to develop into strong hurricanes in the Atlantic during the warm phase.

2.2.1.5 Arctic Oscillation (AO)

Arctic Oscillation causes variability in the northern hemisphere through north-south shifts in zonal winds in association with north-south shifts in atmospheric pressure that fluctuate between negative and positive phases. It should be considered separately from North Atlantic Oscillation, as its influence extends across both ocean basins, whereas North Atlantic Oscillation is typically confined to the Atlantic basin[22].

The positive phase – low pressure over the Arctic, and high pressure over the central Atlantic – brings the opposite conditions with strong polar circulation pushing ocean storms farther north and bringing

wetter weather to Alaska, Scotland and Scandinavia, and bringing drier, drought conditions to areas such as California, Spain and the Middle East.[23] The negative phase brings higher-than-normal pressure over the Arctic and low in the mid-latitudes, which leads to weaker Westerlies that allow cold Arctic air to push into the Midwestern United States and Western Europe, bringing a cold winter to those areas, and storms to the Mediterranean.

2.2.1.6 Arctic Sea Ice

Sea ice forms and melts in sea water, and should be considered separately from land-based ice in the region when thinking about components of the climate system. It begins to form at around —1.8˚C in small disc-like sheets that grow and merge together to form ice floes that can cover on average 25 million km^2.[24] As the ice forms, salt is expelled, forming saltier, denser water that sinks, driving a component of the global sea circulation system.

Surface coverage of sea ice in the Arctic can indicate changes in the global climate system, and reinforce those changes themselves as it has a role in a number of global processes, whether this is the diffusion of solar energy (white ice reflects more sunlight than sea water), atmosphere and ocean circulation (depending on whether there is more or less moisture available), or playing a part in heat exchange. The reduction in sea-ice cover in recent years has seen an increase in the heat flux from the ocean to atmosphere in autumn and early winter, which has increased air temperature, moisture and cloud cover in the region.[25]

2.2.1.7 Australian Blocking Index (BI)

Blocking highs are strong high pressure systems that form further south than usual and remain near stationary for an extended period of time, essentially blocking the normal west to east progression of weather systems across southern Australia. They typically form across the Tasman Sea and Southwest Pacific[26], and are identified by a blocking index created by the Australian Bureau of Meteorology.[27, 28]

Blocking highs are often associated with a cut-off low which may form to the north of the blocking high, the two systems interacting to create a blocking pattern. As frontal systems approach the blocking high, they slow down, weaken, and are pushed to the south of the block. Blocking highs can affect large areas, and have been known to cover all of southern Australia. They can occur at any time of year, last from several days to several weeks and, depending on their location and strength and how the block interacts with the systems around it, can produce hot spells, cold spells, dry conditions or wet conditions.[29]

2.2.1.8 Boreal Summer Intraseasonal Oscillation (BSISO)

Boreal Summer Intraseasonal Oscillation is a large and slow-moving envelope of cloud systems and precipitation, and is one of the prominent modes of tropical intraseasonal variability from May-November[30], with the related Madden-Julian Oscillation dominating from December until April[31]. During the boreal summer, the main centres of convective variability tend to move eastwards along the equator as a result of the Madden-Julian Oscillation phase, and then head northwards over the Indian Ocean and western Pacific areas as a result of surface heat fluxes[32]. This sequence drives the transportation of heat and momentum in its cloud systems across the region, forming a northwest-southeast tilted rain band[33]. However, this isn't always guaranteed; Boreal Summer Intraseasonal Oscillation is very complex, with changes in surrounding or influencing systems varying the strength, speed, and direction, which in turn affect summer monsoon onset and wet (active)/dry (break) phases.[34, 35] These variations can bring unpredictable extreme[36] impacts ranging from flood to drought as a result of variations in monsoon rainfall strength, and can alter the frequency of tropical cyclones and extra-tropical storms.[37, 38]

2.2.1.9 East Atlantic Pattern (EAP)

The East Atlantic Pattern is the second most dominant mode of sea-level pressure in the North Atlantic region, and takes the form of a low-pressure centre in the Northeast Atlantic and a high-pressure centre over North Africa/the Mediterranean Sea[39]. The East Atlantic Pattern subtropical link makes it distinct from North Atlantic Oscillation, although it is structurally similar, which is why it is often described as a southward shift in the North Atlantic Oscillation in existing literature.[40] In the positive phase, the pressure gradient between the two pressure systems results in an intensification of the Westerlies over the central latitudes of the eastern North Atlantic and much of Europe. This pattern brings warmer air to Europe, with increased rainfall seen in Northern Europe as more storms hit the area and drier conditions across southern Europe due to the shift in winds[41].

2.2.1.10 El Niño-Southern Oscillation (ENSO)

El Niño-Southern Oscillation represents the cycle of fluctuation in sea-surface temperatures circulation that occurs across the equatorial Pacific Ocean, and dominates climate variability from year to year.[42] This cycle switches from El Niño to La Niña on a timescale of a few years[43], with neutral periods occurring where neither is dominant. The El Niño phase sees a warming of the ocean surface, or above-average sea-surface temperatures in the central and eastern tropical Pacific Ocean. The low-level surface winds, which normally blow from east to west along the equator, weaken, or in

strong El Niño years, reverse their direction and become westerly. In the La Niña phase the opposite occurs, with cooling of the ocean surface resulting in below-average sea-surface temperatures in the central and eastern tropical Pacific Ocean. The normal easterly winds along the equator also become stronger.[44] El Niño events tend to only last for a single cycle from autumn to autumn, but it is not uncommon for multi-year La Niña events to occur as they did in the 1998-2001 period.[45]

The fluctuations in sea-surface temperatures are also coupled with changes in air-pressure systems – the Southern Oscillation part of the name. These changes affect the position and intensity of the jet streams, which change the tracks and intensity of storms. The negative phase of the Southern Oscillation occurs during El Niño, and sees abnormally high air pressure covering Indonesia and the western tropical Pacific, along with lower than normal pressure covering the eastern tropical Pacific. The positive phase, which occurs during La Niña, brings abnormally low pressure to Indonesia and the western tropical Pacific, and abnormally high pressure to the eastern tropical Pacific.[46]

2.2.1.11 Indian Ocean Dipole (IOD)

Indian Ocean Dipole is a coupled ocean-atmosphere system[a] found in the Indian Ocean[47] that is defined by the difference in sea-surface temperatures between a western pole in the Arabian Sea and an eastern pole in the eastern Indian Ocean, south of Indonesia[48]. The index of the Indian Ocean Dipole is known as the Dipole Mode Index[49]. The positive phase sees lower than average sea-surface temperatures and greater precipitation in the western Indian Ocean region, with corresponding cooling of sea-surface temperatures in the eastern Indian Ocean. This brings drought conditions across Indonesia and Australia, and sees increased rainfall in east Africa. The negative phase of the Indian Ocean Dipole brings opposite conditions, with warmer waters and greater precipitation in the eastern Indian Ocean, and cooler and drier conditions in the west.[50]

2.2.1.12 Interdecadal Pacific Oscillation (IPO)

The Interdecadal Pacific Oscillation[51] is the natural fluctuation between warm and cold temperatures that alternates every few decades, and is a significant source of climate variability in the South West Pacific[52]. Interdecadal Pacific Oscillation covers the entire Pacific Basin, and occurs over 20-23 year time periods, which are determined by oceanic Rossby wave[b] propagation through the extratropics. The positive phase brings warm sea-surface temperature anomalies in the tropics and cold ones over the central and western extratropical Pacific, which brings a significant reduction in the number of tropical storms over the North Atlantic and an increase in the eastern North Pacific that is mainly driven by changes in wind shear[53]. The negative phase sees cold anomalies in the tropics and warm ones over the central and western extratropical Pacific[54].

Changes in the Interdecadal Pacific Oscillation phase cycle match up with global shifts in sea-surface temperatures, sea-level pressure, temperature and precipitation. It has been described as being an El Niño-Southern Oscillation -like mode that occurs over decadal timescales[55]. The two phases of the Inter-decadal Pacific Oscillation appear to modify the magnitude of year-to-year El Niño-Southern Oscillation precipitation and temperature variability, although a lack of consistent methods and the global scale data source mean that effects are not yet fully understood.[56]

2.2.1.13 Madden-Julian Oscillation (MJO)

The Madden-Julian Oscillation[57, 58] is the major fluctuation in tropical weather on weekly to monthly timescales that takes the form of an eastward moving "pulse" of cloud and rainfall through the Indian and Pacific oceans where the sea surface is warm.[59] The pattern is formed through atmosphere-ocean interactions, with warm seas pushing air up through the atmosphere leading to condensation and rainfall. As the system moves eastwards, the warm air later cools and sinks but on meeting the warm seas tends to dry out, bringing sunny and dry conditions.[60] The cycle takes place over 30-60 days before returning to the starting point much like a spinning wheel travelling along a path, and there can be multiple Madden-Julian Oscillation events within a season[61]. Depending on where the system is in its cycle in terms of enhancing or supressing rainfall,[62] it can modulate the intensity of monsoons; tropical cyclone activity in the Indian, Pacific and Atlantic Oceans; and contribute to the speed of development of El Niño episodes.[63]

2.1.14 North Atlantic Oscillation (NAO)

The North Atlantic Oscillation consists of a see-saw of surface pressure between two points – Iceland and the Azores – that can have large effects on the weather and climate patterns in the surrounding regions by changing the intensity and location of the North Atlantic jet stream[64]. It occurs all year round, however it is particularly dominant during the winter from December to March[65]. In the positive phase of North Atlantic Oscillation there is a stronger-than-normal low pressure system over Iceland, and a stronger-than-normal high pressure system in the Azores, with a

[a] Linked changes of the sea-surface temperatures over the tropical waters and changes in pressure gradients, which in turn influence the air currents above.

[b] Oceanic Rossby waves are large-scale waves within an ocean basin. They have low amplitude/height – centimetres to metres – compared to a long wavelength, which can be of the order of hundreds of kilometres. They may take months to cross an ocean basin.

strong pressure gradient between the two regions[66]. This allows winds from the west to dominate that bring warm air across the Atlantic. This pattern brings mild, stormy and wet winter conditions in northern Europe and eastern US, and cold and dry winter conditions to northern Canada, Greenland and southern Europe.[67] The negative phase sees weaker pressures in both systems, resulting in an even weaker differentiation between the two that generates a blocking effect that adjusts the position of the jet stream. This allows winds that bring cold air from the east and north-east to dominate, bringing cold, dry winters to Europe and the eastern US, and mild and wet winters to northern Canada and the Mediterranean.[68]

2.2.1.15 North Pacific Oscillation (NPO)
The North Pacific Oscillation is the Pacific sector equivalent to the North Atlantic Oscillation and is defined by fluctuations in sea level pressure characterised by high pressure over Hawaii and low pressure in the Gulf of Alaska[69]. It is connected with downstream weather conditions over North America and is a potential mechanism linking extratropical atmospheric variability to El Niño events in the tropical Pacific[70]. North Pacific Oscillation modes are often associated with large regional variations in air temperature and precipitation over North America, sea-surface temperatures in the North Pacific and Bering Sea ice[71].

2.2.1.16 Pacific Decadal Oscillation (PDO)
The Pacific Decadal Oscillation is the dominant year-round pattern of monthly North Pacific sea-surface temperature variability. It is a complex combination of different physical processes, made up of both remote tropical forcing and local North Pacific atmosphere/ocean interactions operating over different timescales to drive similar Pacific Decadal Oscillation -like sea-surface temperature anomaly patterns[72]. Shifts in the phase alter the upper level atmospheric winds and can have significant implications for global climate, affecting Pacific and Atlantic hurricane activity, droughts and flooding around the Pacific basin, productivity of marine ecosystems, and global land temperature patterns.[73]

2.2.1.17 Pacific North America (PNA) pattern
The Pacific-North America pattern is described as a Rossby wave train of anomalies in the geopotential height field, with four alternating pressure zones that form an arc from the north eastern Pacific across to the south-eastern US[74]. It influences winter air temperature and precipitation over much of western North America, as well as Arctic sea ice in the Pacific sector, by affecting the strength and position of the jet stream that delivers weather to the region.[75] The positive phase is associated with an enhanced East Asian jet stream and with an eastward shift in the jet exit region toward the western United States. The negative phase is associated with a westward retraction of that jet stream toward eastern Asia, blocking activity over the high latitudes of the North pacific, and a strong split-flow configuration over the central North Pacific.[76] Although it is an independent mode of climate variability, it also responds to changes in sea surface temperatures, which is reflected by El Niño-Southern Oscillation, with phases matching up with the cycle – positive Pacific North America pattern/El Niño and negative Pacific North America pattern/La Niña.[77]

2.2.1.18 Quasi-biennial Oscillation (QBO)
Quasi-biennial Oscillation is the cycle of wind direction in the stratosphere at heights of 20-40km that blows in a continuous circuit around the Earth.[78] These winds may weaken and change direction, switching from east-west and west-east roughly every 14 months.[79] The cycle is driven by waves descending between the troposphere and stratosphere, breaking and transferring energy and momentum between the layers and enforcing wind direction. Westerlies tend to move down faster and easterlies tend to be stronger so the cycle varies between the two directions.[80] Quasi-biennial Oscillation can affect the strength of other systems, such as the westerly phase enhancing positive phases of the North Atlantic Oscillation, increasing the strength of the jet stream and storms that form along the track,[81] and affecting tropical storm development by modulating the cloud environment.[82]

2.2.1.19 Rossby Waves/Other Planetary Waves
Rossby Waves occur at mid-latitudes, and normally take the form of waves hundreds of kilometres long that are continuous around the hemisphere and orbit both poles.[83] Due to their large wavelengths, the patterns of flow can connect regions separated by great distances – they define the essence of teleconnections in their structure and effects.[84] They form in large part due to the structure of the relatively thin atmosphere in relation to the size of the Earth, with energy and circulation patterns able to build up from side to side/horizontally much more easily than up-down/vertical winds.[85] Rossby Waves are characterised by cold troughs and warm ridges, and best develop between about 700mb and 200mb; they can be almost-stationary or travel slowly depending on their thermal structure.[86] When they swing north, their massive size and momentum sucks warm air from the tropics into Europe, Russia, or the US, and when they swing south, they do the same thing with cold air from the Arctic.[87]

2.2.1.20 Scandinavia Pattern (SCP)
The Scandinavia pattern is a difference in atmospheric pressure systems between Scandinavia and opposing centres over south-eastern Europe and Russia/

Mongolia.[88] The positive phase of the Scandinavia pattern sees high pressure – often as blocking systems – over Scandinavia that brings dry conditions, and low pressure in the southern systems, often bringing cooler temperatures across central Russia and Western Europe, as well as high levels of precipitation across central and southern Europe.[89] Depending on the season, this may fall as increased rainfall in the summer or heavy snowfall in the winter. The negative phase sees the opposite occur, with high levels of precipitation across Scandinavia and dry conditions in Western Europe.[90]

2.2.1.21 Southern Oscillation Index (SOI)

The Southern Oscillation is a pressure anomaly over the Indian and South Pacific Oceans, switching between cycles around every 2.33 years that can be used to give an indication of how an El Niño (negative phase) or La Niña (positive phase) event is developing, and how strong it might be,[91] as it corresponds very well with changes in ocean temperatures across the eastern tropical Pacific.[92]

2.2.1.22 Volcanoes

Volcanic activity can affect the Earth's climate systems through the ejection of ash and gases into the atmosphere during eruptions, forming clouds or plumes that block sunlight.[93] Cooling is most often associated with volcanic eruptions, with ash and sulphur-rich aerosols causing the most significant effects through the creation of atmospheric haze.[94] As material is thrown up into the upper layers, sulphur dioxide is converted to sulfuric acid as it combines with moisture, forming fine sulphate aerosols; it is these aerosols that increase the reflection of radiation from the sun back into space, leading to cooling of the surface.[95] In the stratosphere, absorption of the direct solar energy and infrared radiation escaping from the surface and troposphere, results in stratospheric heating despite the reduction in solar heating from ozone. These effects may persist for 1-3 years, after which growth and coagulation lead to sedimentation and recirculation of the aerosol into the troposphere.[96]

The geographical location of where eruptions take place can also have an impact, as eruptions along the tropics see greater atmospheric circulation and distribution of aerosols; evidence suggests that the Krakatau (1883) and Tambura (1815) eruptions, may have cooled the atmosphere by about 0.3˚C and 0.4-0.7˚C respectively.[97]

2.3 Identifying key climate drivers

For each region-peril-driver combination, a review of academic literature was undertaken to establish background information on the seasonality, geography and the general characteristics of the relationship between global drivers.

From this analysis, nine key drivers were identified according to their timescale of influence. This involved challenging the evidence through a series of staged queries and expert scientific review of the findings, as summarised below:

1 For the defined perils, the relevant climate drivers were identified from research studies to:
   - Determine the nature of the relationship between the driver and the peril. Does the mode increase or decrease the risk of the peril? Can this be quantified?
   - Determine the robustness of these relationships: What is the range of studies in which the relationship has been identified? Is the mechanism understood?

2 For the climate drivers relevant to the significant perils, the nature of the relationships between climate drivers were determined and the robustness of these relationships assessed:
   - Does one driver being active make another driver more likely? Can this be quantified?

3 The dependencies between different perils and regions were analysed. Those perils that are most likely to exhibit a dependent relationship were determined from the matrices, i.e. those related to the same mode of variability or different modes with a significant dependency on each other.

Given the requirement that connections between global extremes are characterised on an annual basis, to align with decision-making timescales in the reinsurance industry, drivers such as the Madden-Julian Oscillation and Boreal Summer Intraseasonal Oscillation that operate on weekly to monthly scales are considered unlikely to provide a significant source of peril-peril connectivity once their impacts are integrated over a year.[98, 99, 100] Other drivers, namely the Pacific Decadal Oscillation, Inter-decadal Pacific Oscillation and Atlantic Multi-decadal Oscillation, operate over the course of decades or more and are similarly not expected to provide an appropriate source of temporal connectivity (*see Table 2, p11*).[101, 102, 103]

There are additional specific reasons for exclusion from the final list:

- The Atlantic Meridional Mode interacts with both the North Atlantic Oscillation and El Niño-Southern Oscillation[104] such that its variability is likely captured by the latter two drivers
- The Southern Oscillation Index essentially provides a southern hemisphere-specific indexed measure of the phase of El Niño-Southern Oscillation[105] and can be captured in the choice of El Niño-Southern Oscillation Index

- The Australian Blocking Index variability is likely to be captured by other southern hemisphere dominant drivers
- No significant correlations were found for the Quasi-Biennial Oscillation

Connections between African Easterly Waves and Rossby Waves are typically discussed in the context of providing mechanisms to connect drivers with particular regions of the Earth, whilst Arctic sea ice and volcanic eruptions are not typically linked to specific regional perils. In the latter case, although causal relationships have been identified, data is usually insufficient to be statistically conclusive.[106, 107, 108] The quantity of available literature relating drivers to the perils of interest also contributed to the decision to prioritise some drivers over others.

As a result of this analysis, the final list of considered drivers becomes:

- El Niño-Southern Oscillation/Southern Oscillation Index
- Arctic Oscillation
- Antarctic Oscillation/Southern Annular Mode
- North Atlantic Oscillation
- North Pacific Oscillation
- Pacific North America pattern
- East Atlantic Pattern
- Scandinavian Pattern
- Indian Ocean Dipole pattern

This facilitates the creation of a matrix of linkages (*see Table 3, p22*) describing the hazard dependency structure that can used to inform understanding of risk.

2.4 Simulating key climate drivers

The first modelling component was to produce suitable simulations of each of the nine key drivers. A statistical model was developed that incorporated information on driver seasonality, including lagged and non-lagged connections, with statistical simulations of driver time series based on Autoregressive–moving-average (ARMA) models. Two-step exploratory analysis, looking first at plots of auto-correlation functions and then plots of cross-correlation functions, revealed that there was non-negligible autocorrelation in each driver, but also dependence of drivers on lagged values of other drivers. (*See Appendix A for full details of how the mathematical model was constructed.*)

To account for driver interaction, the process by which the states of one driver may influence the state of another, a hierarchical model process was created, constructed in a cascading fashion (*see Figure 2, p18*). The North Atlantic Oscillation, East Atlantic Pattern, Scandinavian Pattern and Pacific North America pattern are by construction mathematically independent[109] so these underpin driver modelling (although the study found there to be some dependency of the East Atlantic Pattern on past values of the other three). For the purpose of this model, North Atlantic Oscillation, Scandinavian Pattern and Pacific North America pattern have no dependence on any other drivers. For reasons of parsimony, auto-regressive time series models were first considered, leaving the use of the more complex autoregressive–moving-average models only if deemed necessary. For the initial three drivers, an AR(1) (Autoregressive) model was sufficient. The order of construction of subsequent drivers was principally based on the expected order of influence (after first accounting for the East Atlantic Pattern dependency) starting with El Niño-Southern Oscillation. By making drivers depend on the state of each other, the model attempts to retain a realistic representation of the co-varying nature of interaction between teleconnection phases without the need for a dynamic model.

The full statistical specification of the driver model is shown in Appendix A2 and the use of the process to determine the model for each driver is illustrated for the El Niño-Southern Oscillation (*Box 1, p19*). Two stages were carried out in each case to both establish the nature of autocorrelation, and to establish the nature of cross-correlation. These two steps were then repeated for the construction of each of the remaining drivers until all remaining models had been constructed.

Figure 2: Hierarchical structure of driver model

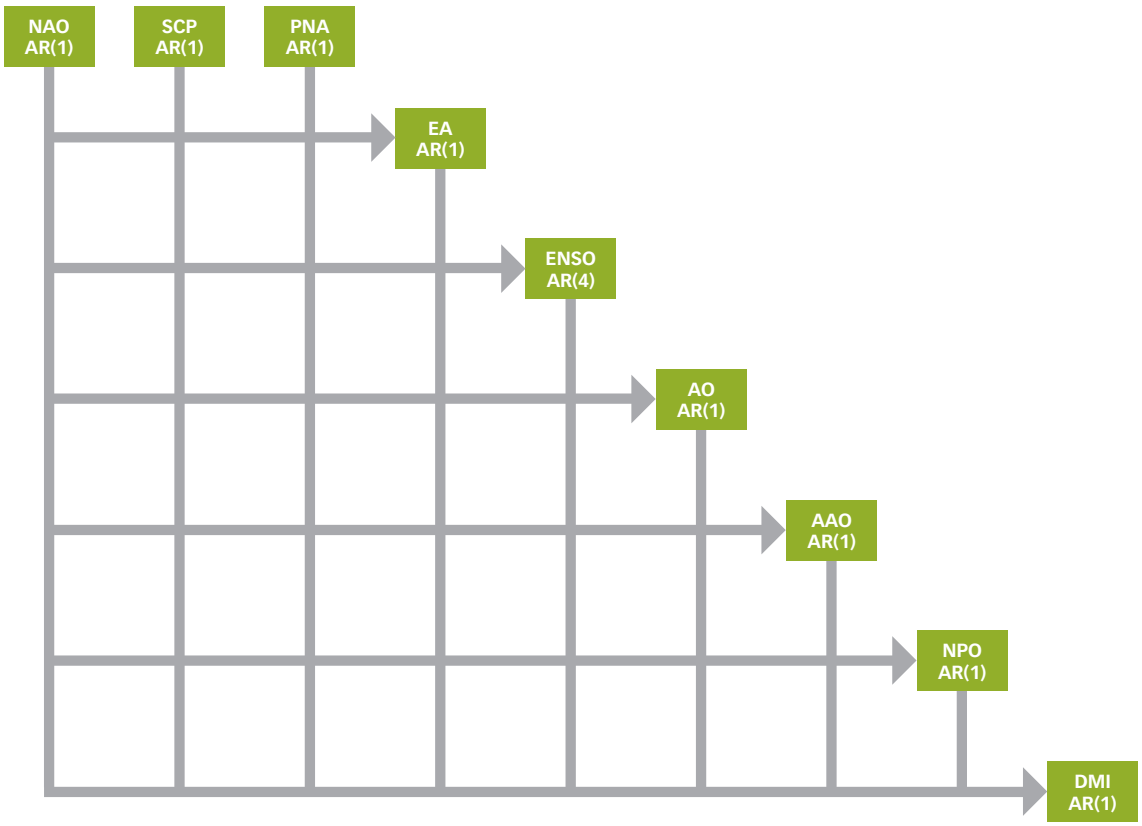

Source: Lloyd's.

An arrow from one driver to another indicates that the former influences the latter but not vice versa. North Atlantic Oscillation, Scandinavian Pattern and Pacific North America pattern are simulated as independent Auto Regressive (AR(1)) processes. The other drivers are all influenced by their own lagged values (AR processes) but also the values of the other drivers higher up the hierarchy. The base AR process is indicated under each driver (*See Section 2.2.1 for the driver descriptions*).

Box 1: Determine El Niño-Southern Oscillation model (example)

Figure 3: Autocorrelation of ENSO time series

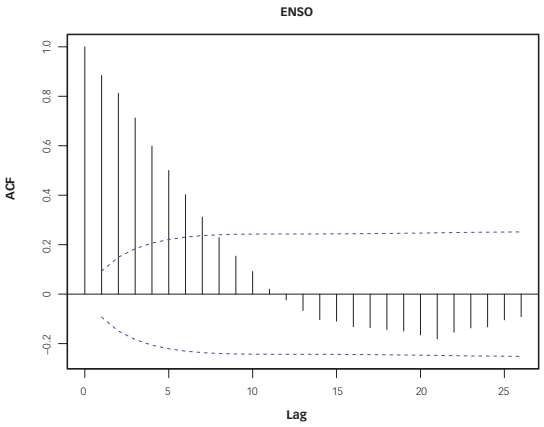

Source: Met Office.

The dashed blue line represents the level above which lags are considered significant. In this case, seven lags are significant.

Developing the El Niño-Southern Oscillation model as an example, the Met Office chose the Bivariate ENSO Timeseries (BEST) Index,[110] which incorporates both sea-surface temperatures, as measured by Nino 3.4, and the Southern Oscillation Index as the model index. An Autocorrelation Function plot of this time series (*see Figure 3, left*) shows there is a significant degree of autocorrelation of up to seven lags. However, testing sequentially higher-order AR models using a Ljung–Box test statistic[c, 111, 112] showed that an AR(4) model sufficiently described the El Niño-Southern Oscillation time series, such that the residuals between the AR(4) model and the original El Niño-Southern Oscillation series are considered independent and identically distributed. Figure 4 (*below*) compares the test statistics of an AR(1) and AR(4) model for the El Niño Southern Oscillation index.

Figure 4: Comparison of test-statistics for an AR(1) (left) and AR(4) (right) model of the El Niño-Southern Oscillation time series used in this study

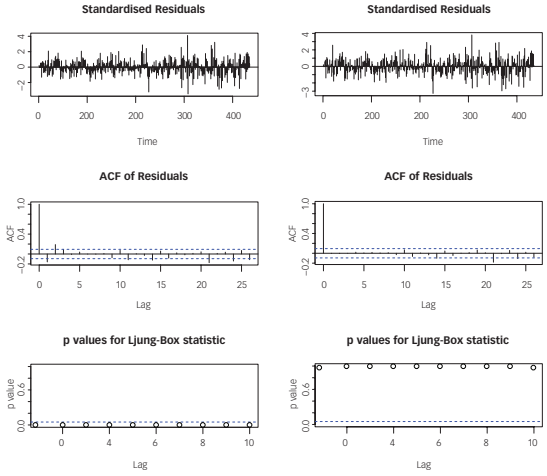

In this case the residual of the AR(1) model still contains a degree of auto-correlation. Investigating successively higher order AR models reveals that an AR(4) model is sufficiently parsimonious to simulate the mthodology's El Niño-Southern Oscillation time series.

Finally, assessment of cross correlation function plots of the El Niño-Southern Oscillation index with each of the northern hemisphere drivers (North Atlantic Oscillation, Scandinavian Pattern, East Atlantic Pattern and Pacific North America Pattern) revealed there to be degrees of correlation with the Pacific North America pattern and North Atlantic Oscillation. Using Z-tests[d, 113] to assess the significance of successively higher Pacific North America pattern and North Atlantic Oscillation lags, found lags of up to seven months to be significant.

The form of the final model is as follows, where Y_t refers to the El Niño-Southern Oscillation peril index at time t (*see Appendix A1 for further details*).

$$Y_t = \alpha + \sum_{i=1}^{4} \phi_i \, Y_{t-i} + \beta_1 \, NAO_t + \beta_2 \, EA_t + \beta_3 \, SCP_t + \beta_4 \, PNA_t + \sum_{j=1}^{7} \gamma_j \, NAO_{t-j} + \sum_{k=1}^{7} \delta_k \, PNA_{t-k} + \epsilon_t$$

[c] Ljung-Box test statistic tests whether a series of observations over time are random and independent.
[d] The Z-test is a hypothesis test based on the Z-statistic, which follows the standard normal distribution under the null hypothesis.

An example of simulated time-series for each of the nine drivers is shown in Figure 5 (*below*). Note that the simulations of the synthetic time series are simulated on a monthly time scale, starting from an appropriate index value taken from the real driver index to facilitate driver interdependence. Whilst this encourages the development of synthetic driver time series with interdependence that mimics reality, this also implies that the choice of driver index will have an influence on driver interactions.

Figure 5: Simulated time series for the nine key drivers for an arbitrary 35-year period

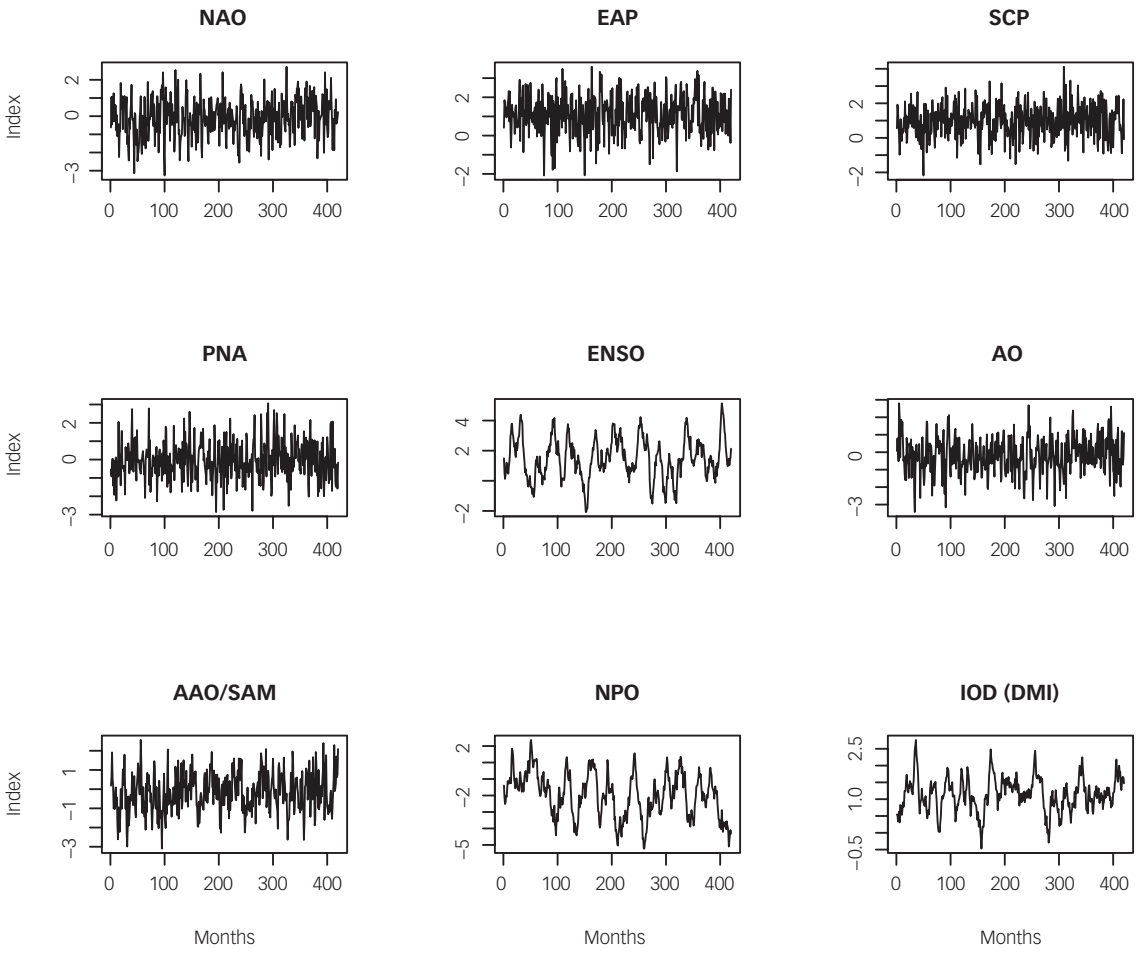

Simulations are based on autoregressive–moving-average models and seek to respect driver interdependence.

The resulting correlation structure between the drivers is shown in Table 3 (*see p22*). Despite the imposed links between some drivers the resulting linear correlation is still small. Some drivers show material correlations between one another.

2.5 Simulating region-peril indices

With suitable driver simulations in place, the connections between each of the nine key drivers and the 16 peril regions were extracted from a further review of scientific literature. Table 3 (*see p22*) summarises the sign, strength and significance of these relationships, defined by a correlation coefficient[e], between drivers and perils. The evidence was evaluated to identify common drivers and their relationships for each pair of perils (known as a peril-peril pair).

The assessment of evidence, in the form of peer-reviewed journal articles, can often result in conflicting views of the dynamic mechanism or correlation between drivers and perils, so it was necessary to assess both the level of agreement between journal articles and estimate a measure of correlation between a driver and peril. Details of driver-peril connections where there was no statistically significant result, or in cases where the strength of a paper's argument was assessed to be insufficient or inapplicable to this study, were not included in the following analysis. Note that in the case of flooding, it was assumed that studies investigating extreme rainfall serve as a suitable proxy where literature specifically investigating flooding is not available.

Where multiple correlation coefficients were suggested, a mean of all values was taken by applying a Fisher z-transform. Where there was evidence of a correlation but a coefficient was not given, a best estimate was provided based on expert judgement and discussion with other peers in the field. All peril-driver correlations were derived from the best available data, but are limited by the robustness of the underlying studies. In most cases, this is directly related to data availability, but certain assumptions had to be made when linking large geographic areas with what are, for the most part, small and frequently convective scale meteorological processes. It is recognised that there is frequently substantial uncertainty associated with even the most robust correlation results but it was decided to omit these in recognition that it should be implicitly accepted that the atmosphere is a complex and chaotic system. Incorporating uncertainty measures at this stage would simply mask any meaningful later results and put too much emphasis on the limitations of past studies.

Some drivers only influence a region-peril for certain months of the year i.e. their effect is seasonal in some cases. For example, the El Niño-Southern Oscillation index only influences Australian flood between September and December inclusive. A table describing the seasonality can be found in Appendix B (*see p42*).

With the underlying correlations identified, a second model component was required that could simulate the interactions of two perils with one shared driver, but also the more complex case of a set of perils with two or more shared drivers (*see Figure 6, p23*). In the latter case, each driver potentially modulates the other, in addition to modulating the peril. Not accounting for this driver-driver interaction may result in the under-estimation of a peril-peril connection in the case where the drivers reinforce each other, or over-estimate where drivers are mutually diminished. Each peril and its associated driver(s) are assumed to follow a multivariate Normal distribution whose variance-covariance matrix contains the correlation coefficients of Table 3 (*see p22*). The size of the two-dimensional covariance matrix is determined by the number of drivers that influence each peril region. A peril time series can then be derived assuming it follows a multivariate Normal distribution. Once each synthetic peril time series is constructed, the evaluation of a peril-peril correlation is found by calculating the Pearson correlation coefficient between two peril time series.

To mitigate uncertainty arising from the short historical period of data (on which the driver time-series models are based), this process was repeated 10,000 times using a Monte Carlo simulation. By simulating various plausible realisations of the drivers, the methodology aims to propagate the uncertainty arising from only having a short historical data set to the estimates of the peril-peril correlations. Rather than providing a single correlation value for each peril-peril correlation, the methodology also provides a confidence interval expressing the uncertainty in only having a short historical data set of drivers.

The mean of the 10,000 correlation values are taken as the final correlation assessment. Correlation significance is assessed by identifying those means that are significantly different from zero at the 90% confidence level (i.e. where the 5th to 95th percentile range does not include zero) and the 68% confidence level. Figure 7 (*see p23*) compares the modelling output in the form of kernel density estimates for two events. Full results from the peril-peril correlation simulations are shown in Section 3 (*see p24*).

[e] A correlation coefficient is a quantification of the statistical association between two random variables. In this case, any reference to a correlation coefficient implies the use of a Pearson correlation coefficient that measures the strength of a linear relationship between two variables. This can be value between +1 and -1, where a value of 0 implies no connection between two variables and a value of +/- 1 implies total positive/negative dependence.

Table 3: Summary of peril-driver interactions using correlation coefficients derived from peer-reviewed journal articles.

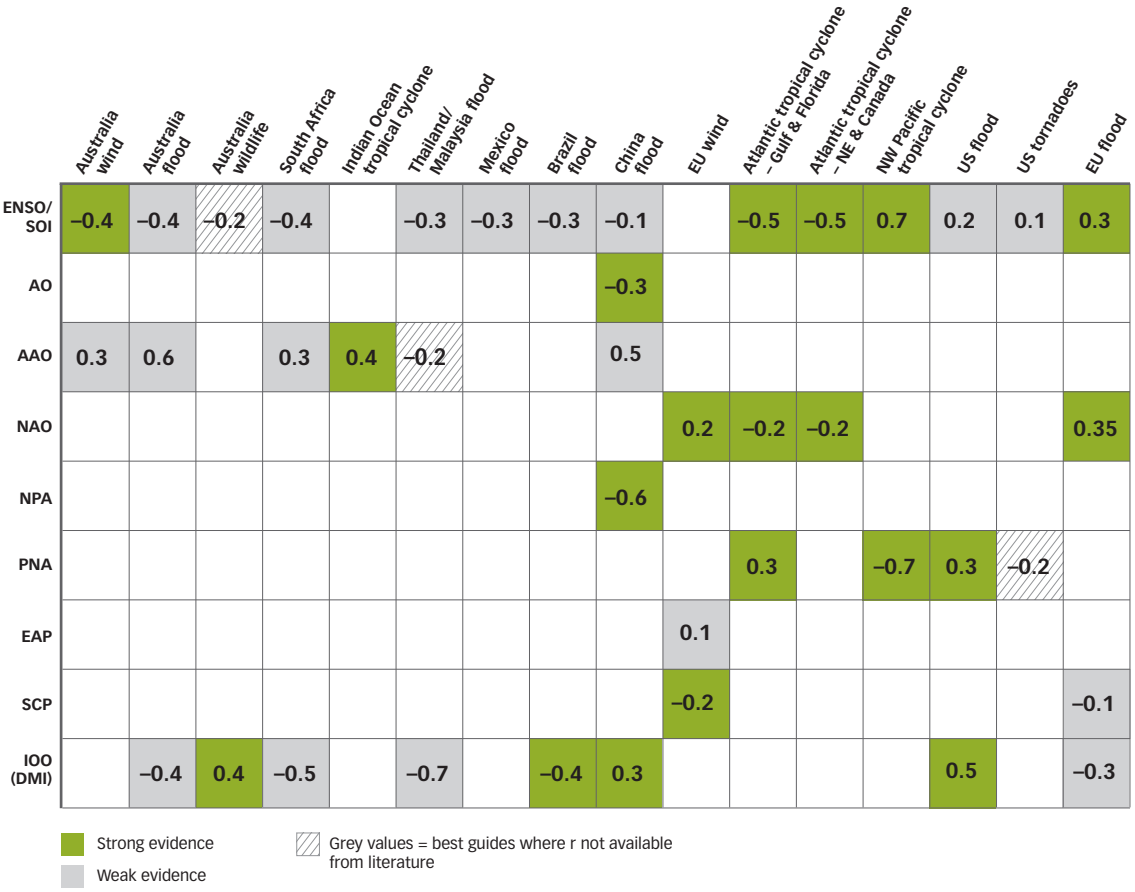

Source: Met Office

Where multiple correlation coefficients are suggested, a mean of all values is taken using a Fisher z-transform. Where there is evidence of a correlation, but a coefficient is not given, the study provides a best guess (grey numbers). The strength of the evidence supporting each coefficient is represented by cell shading. Strong evidence (dark grey shading) is where multiple papers corroborate similar findings with multiple statistically significant correlations between peril and driver. Additionally, the connection between the peril and meteorology is clear. Weak evidence (light grey shading) is defined: a) where the study found numerous papers with conflicting evidence of driver-peril correlations, typically defined where papers find correlations of opposite sign; b) or significant and insignificant correlations; c) or papers where no significant correlation is found, but where a dynamic connection between the driver and peril is postulated; d) or the connection between the peril and the underlying meteorology is unclear, even in the presence of an observed correlation. Note that the study does not show a correlation where there is either no significant correlation or where no evidence is found to support or connection. Correlation entries reflect best available data at the time of publication.

Figure 6: Illustration of the model for two perils (Gulf-Florida tropical cyclone and European flood)

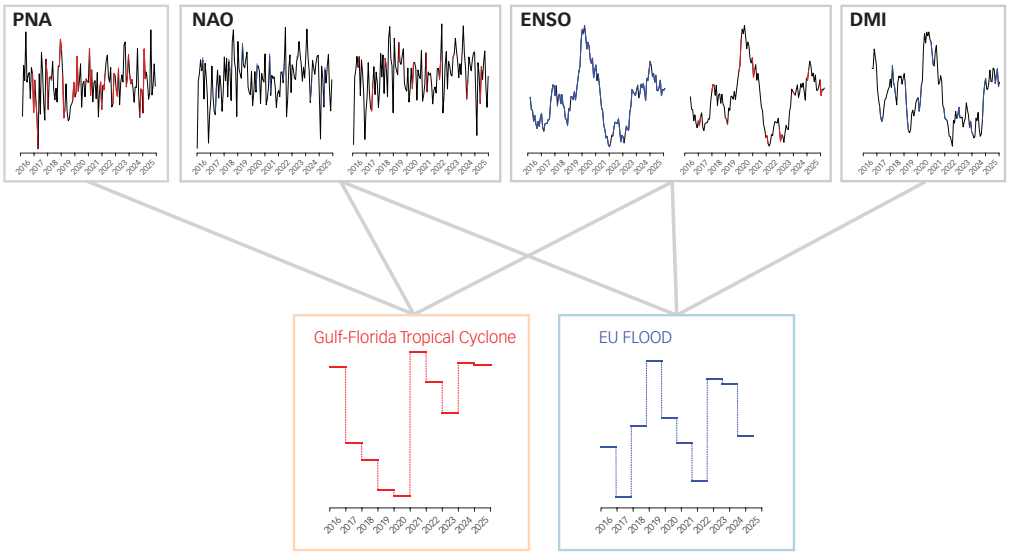

Source: Lloyd's.

The two perils are each influenced by multiple drivers. Specifically Gulf-Florida tropical cyclone by Pacific North America pattern, North Atlantic Oscillation and El Niño-Southern Oscillation and European flood by North Atlantic Oscillation, El Niño-Southern Oscillation and Dipole Mode Index. Note that the El Niño-Southern Oscillation index influences European Flood throughout the year, but influences Gulf-Florida Tropical Cyclone only from August to October inclusive.

Finally, to assess the robustness of these uncertainty estimates, the whole simulation process (including running Monte Carlo simulations for each peril-peril pair) undergoes 100 repetitions. Significant pairs are compared in each instance. The Met Office makes further comment of these results in the Model results described in the following section.

Figure 7: Kernel density estimates showing the sampling uncertainty of the correlation estimates for two events

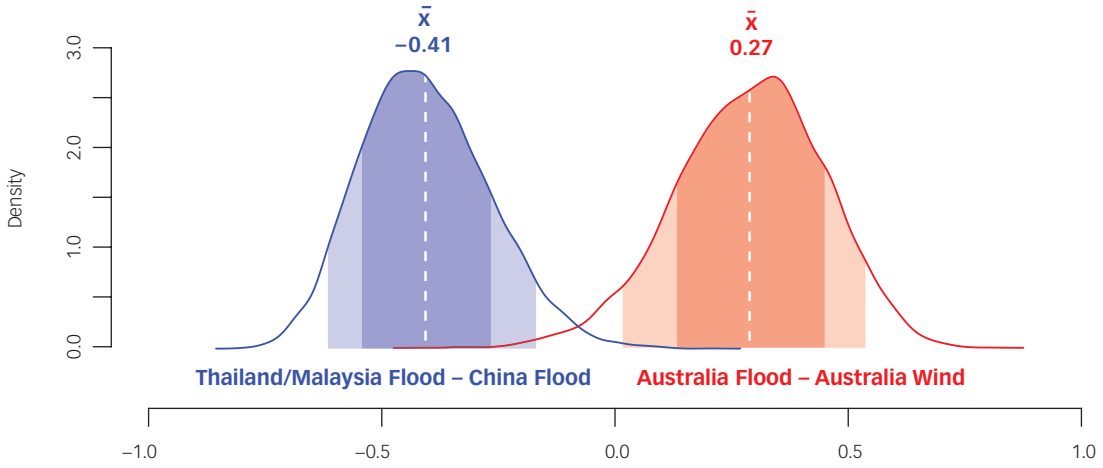

Source: Met Office.

Shaded areas represent the limits of the 90% and 68% confidence intervals. The position of the mean correlation values are shown by the white dashed line. Note that for each comparison, the tails of the distributions suggest that there is a small chance that on some occasions the peril-peril pairs may demonstrate opposite correlations to those reflected in their mean value.

3 Model results

A summary of results from the peril-peril correlation modelling are shown in Figure 8 (*below*). This matrix represents the mean correlations value obtained from the 10,000 Monte Carlo simulations. The spread of values obtained from the Monte Carlo analysis is used to assess if the mean value is significantly different to zero by examining the locations of the 5th and 95th percentiles. If this range does not overlap zero, the study concludes the means are significantly different to zero with 90% confidence. This process is repeated for a range of one standard deviation, providing a second assessment at 68% confidence. Out of 100 repetitions of the complete modelling process, the results significant at either 90% or 68% confidence are significant in at least 97 out of 100 replications.

Figure 8: Matrix of correlations for the full set of perils

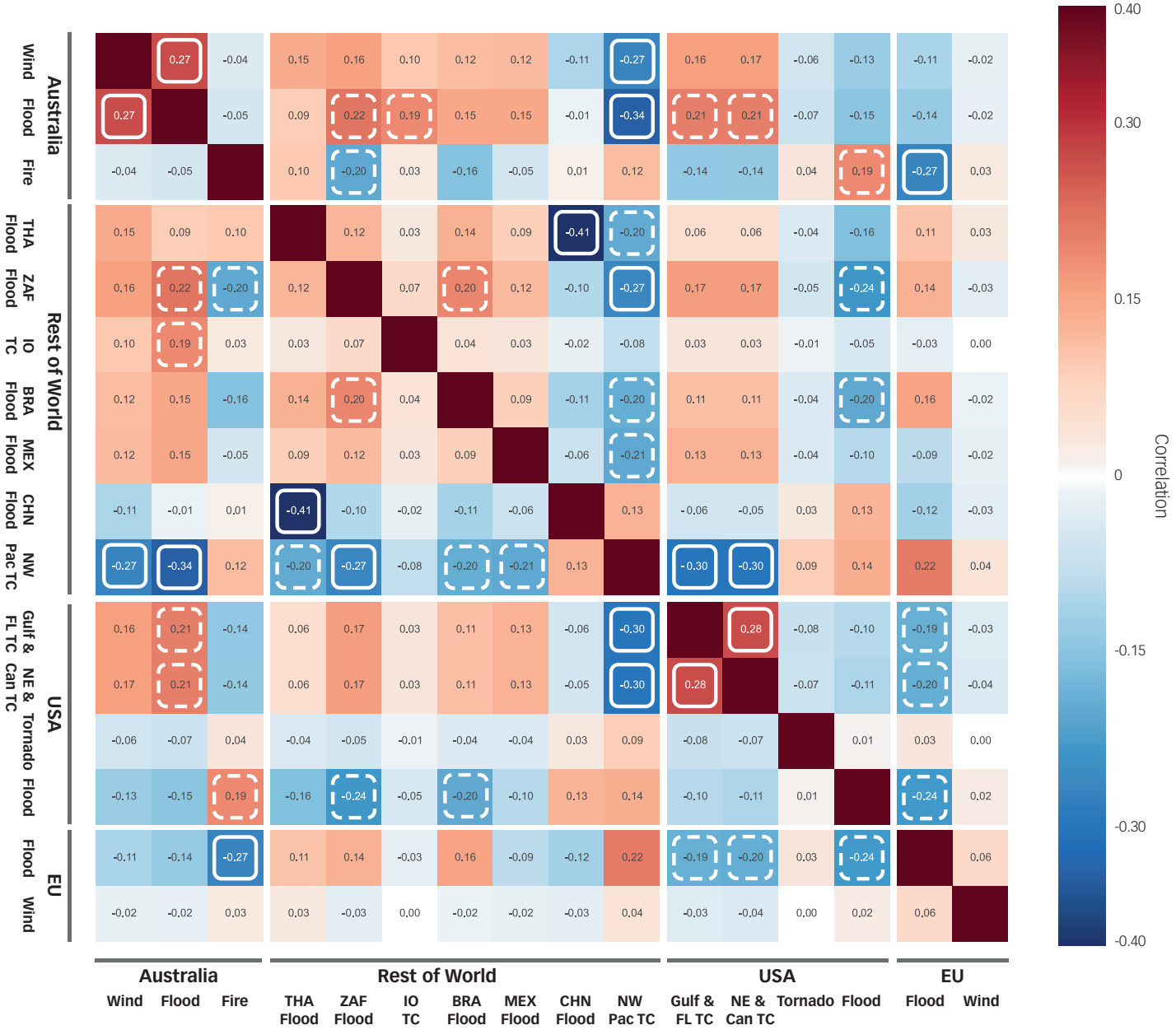

Source: Met Office

Significantly different to zero: White box = 90% confidence; Broken white box = 68% confidence.

Connections that are significant at 90% are highlighted with a solid white box. Connections that are significant at 68% are highlighted with a broken white box.

A summary of those results that are significant at 90% are highlighted in Figure 9 (*below*). This shows the full spread of correlation values found during the Monte Carlo process, as well as the limits of the 90% and 68% confidence intervals.

Figure 9: Box plots of the nine significant peril-peril correlations with associated uncertainty bounds at the 90% and 68% level

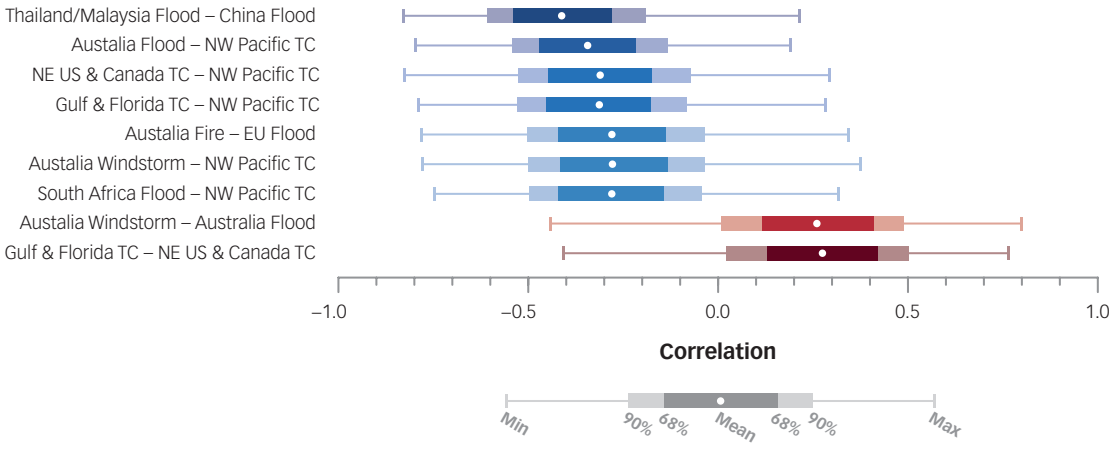

Source: Met Office

The lines extending from either side of the box represent the maximum and minimum simulated correlation values for each peril pair based on 10,000 Monte Carlo simulations.

Significant results at both 90% and 68% are visualised in map form in Figure 10 (*below*). Here, the thickness of lines connecting two peril regions represents the strength of the correlation. Correlations significant at 68% are represented by dashed lines.

Figure 10: Map of key correlations between perils

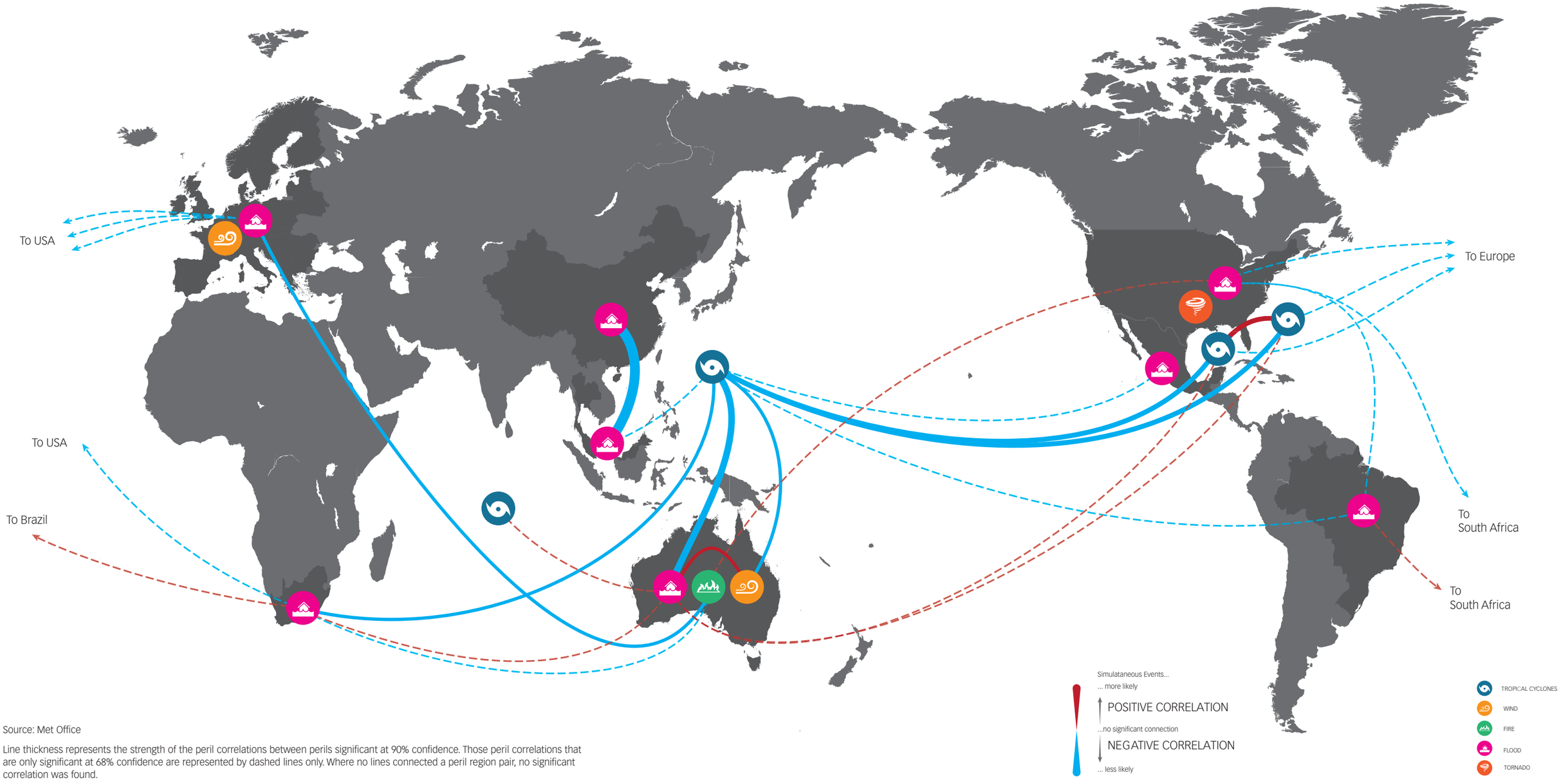

Source: Met Office

Line thickness represents the strength of the peril correlations between perils significant at 90% confidence. Those peril correlations that are only significant at 68% confidence are represented by dashed lines only. Where no lines connected a peril region pair, no significant correlation was found.

Most peril connections appear to be influenced by the state of El Niño-Southern Oscillation, which affects 14 of the 16 peril regions. However, there is not always uniform agreement on the mechanism of this influence, particularly for US tornadoes, which remain relatively poorly understood, and China flooding, where the relationship between rainfall and surface run-off is unclear[114] principally due to rapid urbanisation and other human activities that are changing land-use properties. European windstorms and Indian Ocean tropical cyclones are the only perils without clear evidence of El Niño-Southern Oscillation influence in current literature, although some authors suggest a link between tropical moisture transport and North Atlantic storm intensification,[115] and recent research suggests that El Niño-Southern Oscillation may modulate the North Atlantic Oscillation[116, 117] (although the stationarity of this connection is unclear[118]). This continues to be an area of active research. For Indian Ocean tropical cyclones, although there is a well understood El Niño-Southern Oscillation influence, El Niño-Southern Oscillation shifts the location of tropical cyclone initiation rather than induces a change in tropical cyclone frequency.[119, 120, 121]

Of those peril-peril combinations that are significant at 90%, connections with North West Pacific tropical cyclones are most numerous (five out of 15). The analysis suggests this is primarily due to its very strong (positive) correlation with El Niño-Southern Oscillation that links it to other El Niño-Southern Oscillation -modulated perils. Indeed, northwest Pacific tropical cyclones have the strongest peril-driver correlations of any peril in this study (with El Niño-Southern Oscillation r = 0.7 and Pacific North American Pattern r = – 0.7). The Accumulated Cyclone Energy[f] tends to increase during strong El Niño events as more tropical cyclones form in the southeast western North Pacific[122, 123], therefore allowing longer travelling time before encountering continental land or cooler mid-latitude water. For the Pacific North American Pattern, it is the strong steering flow of its negative phase that results in the strong negative correlation. The steering flow derives from anomalous cyclonic and anticyclonic circulations that intensify at low- and mid-latitudes from East Asia to the North Atlantic respectively, producing south-easterly winds that move tropical cyclones towards Taiwan and mid-latitude coastal regions of Southeast Asia.[124] Only the association between the Indian Ocean Dipole and flooding in Thailand and Malaysia is of equivalent magnitude.

Of the weakest peril-driver correlations, US tornadoes are found to have the weakest link with large-scale drivers principally due to significant regional variation. Enhanced tornado activity has been shown to be associated with anomalously cool Pacific sea surface temperatures (synonymous with La Niña conditions) in the Gulf of Mexico.[125, 126] Significant correlation of tornadoes from March to May with strong December to February El Niño-Southern Oscillation events provides a potential source of predictability. Spatially however, although El Niño conditions see tornadoes decrease in Central US, on the Gulf coast and Florida, El Niño sees a significant increase in tornadoes occurrence[127].

In the context of these findings, it is important to recognise some limitations of the methodology. This assessment is based on the current state of climate dynamics and does not account for possible future change in the Earth's climate system. It is also assumed that any driver-driver interaction in either the form of driver-to-driver enhancement or diminishment is captured by the study's tiered driver simulations. A fully dynamical assessment of these interactions could be addressed in future studies using numerical weather predication models (as discussed in the final study section on future developments).

3.1 Simulating conditional extremes

The peril index in the year is calculated as a draw from a standard normal distribution (mean zero and variance 1). The mean of this distribution, for a simulated year, is determined by an appropriate combination of the driver indices for each peril normalised so that the average peril index over a long time period is zero. This determines the "risk background"; a positive peril index indicates conditions more conducive for the peril to arise and negative less so. The variance of the normal distribution is determined so that, taking account of the additional variance introduced by the relevant driver indices, the overall variance of the peril index is one. Each index reflects the background risk for the given region-peril over time, which can rise and fall in practice for two reasons: (1) the behaviour of the relevant drivers and (2) random effects reflecting other features affecting the background risk. The random effects are chosen by sampling from the specified normal distribution and represent the limits of current scientific understanding (i.e. specific reasons for these random effects are not modelled but it is acknowledged that they are there). Since many peril indices are affected by common drivers this introduces dependency between the peril indices which this model captures.

As noted, the fact that a peril index is high does not automatically imply that an extreme event will occur. The specific details of how to model this residual extreme event uncertainty are arguable; the index could be used to specify a measure of centrality of the distribution (mean,

[f] ACE Index: a metric that combines number, lifetimes and intensities of tropic cyclones.

median or mode) or some other quantile. Therefore, there are a number of ways to generate pseudo insurance claims from the index (*see Appendix A2 for an example*), where the index value is assumed to equate to the loss at a given quantile of the loss distribution.

In Lloyd's experience, a reinsurance contract often suffers a full limit loss in a major event. This implies reduced sensitivity to major losses (i.e. once the contract has paid in full, it cannot pay any more, even if an event is larger). This is not the case for some direct or binder business where losses can continue to increase as events grow in size but for a business with a mix of direct and reinsurance it tends to imply that the sensitivity of the most extreme losses is lower than the more typical losses. As such, Lloyd's has chosen to impose a constraint that, as the peril index grows, the deep tail of the loss distribution grows less quickly than the more frequent losses.

Lloyd's has a catastrophe model that forms part of its internal model and that is based on its syndicates' models (syndicates are groupings of members who come together to underwrite risks that operate in the Lloyd's market). The syndicates' use a variety of approaches to model catastrophes: some use proprietary catastrophe models; others have developed their own models. The Lloyd's model amalgamates relevant parts of the syndicates' models and as such Lloyd's has already modelled views of natural catastrophe risks by peril (known as "marginal distributions"). These are currently combined by independently allocating the ranks of each marginal distribution to all simulations. In order to test the model presented in this study (referred to below as the "drivers-based model" to avoid confusion) in the context of Lloyd's internal model, Lloyd's first created the peril indices then sampled pseudo insurance losses from them in the manner described above. This created a multivariate distribution for each region-peril. These were then grouped where necessary to match the structure of Lloyd's internal model. Finally, the ranks were extracted from the grouped drivers-based-model which captured how each of the region-perils relates to the other. The actual marginal distributions from Lloyd's internal model were then matched so that the ranks are in 1-1 correspondence.

For example, suppose that a pseudo-claim relating to European Windstorm for a given simulation is ranked 154 and within the grouped drivers-based model this relates to rank 2,435 from the North West Pacific Tropical Cyclone claims. Lloyd's would then sort its marginal distributions and find the modelled loss ranked 154 in the European Windstorm distribution and join it together with the loss ranked 2,435 from the North West Pacific Tropical Cyclone distribution. This ensures the rank correlation structure from the drivers-based model is preserved in Lloyd's internal model. Technically speaking, Lloyd's then extracts the copula from the drivers-based model (estimated through simulation) and uses this to combine the marginal distributions (referred to as the "drivers-based copula", below). This shows that the modelled 1 in 200 (*for example*) based on an assumption of independence is statistically no different from the value derived using the drivers-based copula.

Lloyd's has carried out multiple sensitivity tests, particularly using different conditional event sampling distributions, and including where the peril index is in 1-1 correspondence with the arising losses as an extreme sensitivity. In all tested cases, Lloyd's finds no discernible impact compared to an assumption of independence, outside of sampling error.

As noted previously, there is clearly some level of dependency between perils since the global atmosphere and ocean is a coupled dynamical system. But the findings of both the data-driven statistical study (*see Box 2, page 30*) and the drivers-based model, show that the impact of this on insurance capital modelling is negligible given the deep uncertainty surrounding the most extreme events.

As such, Lloyd's concludes that an assumption of independence for the risk groups that it assesses is currently appropriate for use in modelling its natural catastrophe risks.

BOX 2: Is it possible to detect teleconnections from the modelling data alone?

The methodology presented in this study is based on physical reasoning. The drivers are well studied and the dependency structure between them is inferred in previously published scientific papers. The relationship between the drivers and the specified region perils is also based on previously published work.

In addition to working with the Met Office, Lloyd's also commissioned Ed Wheatcroft, a statistics consultant based at the Centre for the Analysis of Time Series at the London School of Economics, to carry out a statistical study based on observed data.

The methodology used in this study focused on the waiting time – the period of time elapsed between consecutive observed events. It tested whether there is evidence that the occurrence of an event in one region peril affects the probability of a second, either in the same or in a different region peril. In the case of the former, this allowed the existence of clustering or anti-clustering to be tested, i.e. whether the occurrence of an event within one region peril made another in quick succession more or less likely.

Based on observed events, the methodology defined samples from the distribution function of observed waiting times (D_0) and compared these to how the distribution would look if consecutive events were independent of each other (D_1). The Kolmogorov-Smirnov test[g] was used to determine whether the probability of the second event is affected by the first. This formally measured the degree of difference between D0 and D1. Standard statistical inference methods were then used to assess whether the level of difference was "significant".

The following tests were carried out - see the full details here: http://www.lloyds.com/weatherconnections-C

1 Determine whether an event in one region peril makes the occurrence of another in the same region peril more or less likely

2 Determine whether an event in one region peril makes the occurrence of another in a different region peril more or less likely

3a Determine whether a given event occurring in any of the region perils makes it more or less likely that another event will occur (this is a globally aggregated view)

3b As for 3a but restricted to major events only

4 Consider whether correlation exists between annual count of different region perils

Key findings

- Experiment 1: No evidence of clustering in US windstorm based on waiting times; some evidence for some of the other perils. Strong evidence of clustering within tornadoes.
- Experiment 2: Some evidence for significant differences in the distribution of one region peril type conditional on a different region peril type in some locations; some of these support the findings of the Met Office study, others don't.
- Experiment 3: The evidence for significant dependency effects was low on a globally aggregated basis and largely disappeared when tornadoes were removed. There is considered to be little evidence for dependency once the focus shifted to the most extreme events. This strengthens the arguments in Section 3.1 that the peril index only relates to the background risk, and further uncertainty remains.
- Experiment 4: Significant correlation between annual counts of region perils was found in some cases. This may be due to increases in the frequency of reported events over time due either to better observing systems or actual changes in the climate over time. Low confidence is ascribed to this result for this reason.
- Experiments 2, 3 and 4: Tornadoes appear so frequently they distorted the analysis and so the evidence has been assessed with and without their inclusion.

See the full details here on the findings listed above. http://www. lloyds.com/weatherconnections-Cs

Conclusions

The study concluded that the short history of observations available made it difficult to draw robust conclusions from the statistics alone. While it is almost certain that some low level of association exists between each of the region-perils, it remains appropriate to use an assumption of independence for modelling purposes.

[g] The Kolmogorov-Smirnov test is a non-parametric, distribution free test, that tries to determine if two datasets differ significantly. It makes no assumption about the distribution of data to do so.

4 Conclusions

Based on the correlation results, what conclusions does the study make about interconnectivity of global weather events?

Conclusion 1: For extreme weather events an assumption of independence is appropriate.

The results of running the methodology in this report through Lloyd's internal model demonstrate that the assumption of independence between weather events in models used by the insurance industry remains appropriate.

Lloyd's has run the proposed model, both with and without the conditional event sampling. In the former case Lloyd's found that the heavy tailed nature of its natural catastrophe models means that no observable correlation exists for extreme events and, as such, a modelling assumption of independence is appropriate.

As regards the latter, event sampling was run as an extreme stress test and effectively assumes that there is a one-to-one correspondence between high peril index levels and the largest extreme events. In this case the study found that US hurricanes and European windstorms are negatively correlated, as are US hurricanes and Pacific typhoons, US hurricanes and the aggregate of perils in the rest of the world are slightly positively correlated. In aggregate, these cancel each other out. This demonstrates that although Lloyd's believes conditional event sampling is the most appropriate model, it is not a critical step to take since even the extreme stress test in which it is omitted does not lead to material impacts on Lloyd's overall modelled catastrophe risk levels.

Figure 11 (*see p32*) helps illustrate why an assumption of independence remains appropriate in the presence of correlated peril indices. The figure compares values of the Northwest Pacific Tropical Cyclone index with the values of the Australian Windstorm index in the same year – some 10,000 pairs of index values are shown in the plot. The correlation between these perils is negative (-0.29) and this can be seen by the tilt in the scatter plot to the left (if they were uncorrelated, the plot would be roughly circular).

A least squares regression line is also shown and this is negatively sloped. The horizontal lines show the expected value of the Australian Windstorm index given that the Northwest Pacific index is larger than a certain value (the notation E(Y|X>1.64) means the expected value of the variable Y given that the X value is greater than 1.64). The peril indices are constructed so they each have variance 1 and mean zero. Taking the red horizontal line as example, that the data shows that the expected value of the Australian index is less than zero (-0.62) when the Northwest Pacific index is larger than 1.64 (which only occurs 5% of the time).

So, consistent with the negative correlation, it is the case that the average Australian index value is lower than normal when the Pacific index is much higher than normal. Note that there is a wide degree of scatter in the Australian index, though. It is still quite possible for the Australian index to take positive values when the Pacific index exceeds 1.64, despite the negative correlation. This is also evidenced by the vertical lines which show the range in which the Australian index falls 90% of the time given the Pacific index exceeds the specified value. The data shows that the width of this range for the unconditional Australian index is 3.27[h] and this narrows only slightly to 3.10 when conditional on the Pacific index exceeding the 1.64 threshold.

In summary, the methodology shows that the Australian index can be expected to fall within -0.62 +/- 1.55 90% of the time when the Pacific index exceeds 1.64. Since the "error" term 1.55 is more than double the average term (-0.62) it is clear that the existence of negative correlation does not mean that both peril indices will always take opposite values. This effect occurs before the conditional event sampling step and illustrates the considerable randomness within the indices themselves.

[h] This is equivalent to conditioning on the Pacific index being greater than its smallest value (4).

Figure 11: Illustration of significant scatter despite correlation between two indices

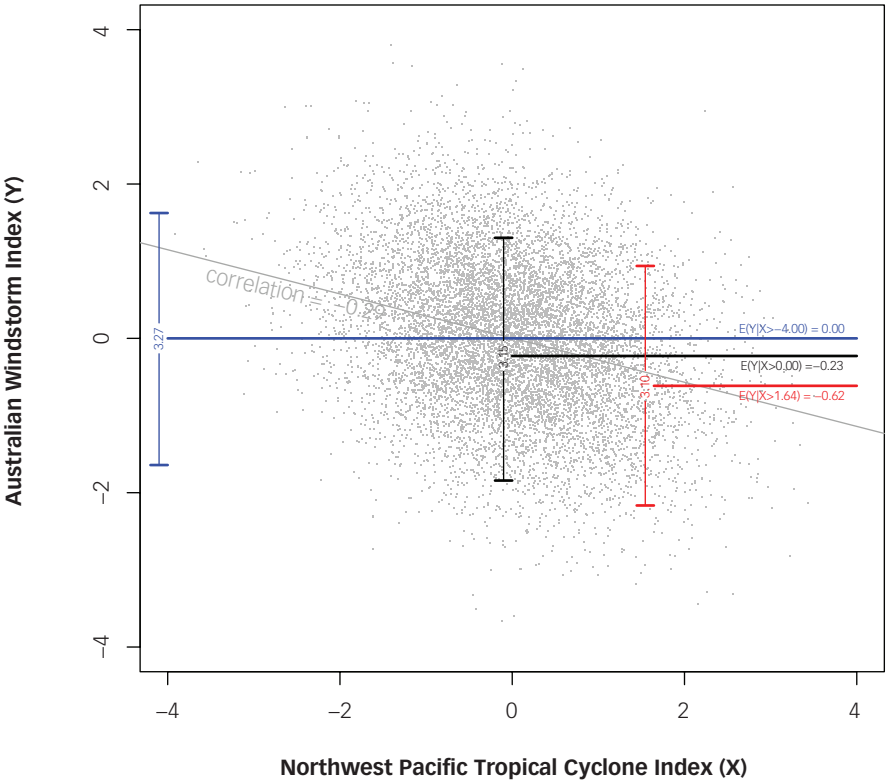

Source: Lloyd's

Conclusion 2: A number of regions show some correlation between weather events but these are not substantial enough to warrant a change in our capital.

While there is some level of dependency between perils, the findings of both the data-driven statistical study (see Section 3.1, Box 2, p30) and the model, presented in the main body of this study, are that the impact of this on insurance capital modelling is negligible. Only nine of the 120 peril correlations analysed in this study showed any significant links, and the links can be both positive and negative. For example, the study confirmed that while the El Niño-Southern Oscillation influences the majority (14 of 16) of regional weather perils, it also reduces the impact of 10 of the 14 perils for three months of the year.

When statisticians speak of a "significant result" this means the result is probably not down to chance; it does not mean the result is "important" or "material" as such labels must be determined by the context and the user. Based on the model presented in this study, the majority (105 of 120) of global peril-peril dependencies are not significantly different from zero. (*See Figure 9, p25 for the full list.*)

Figure 9 shows the uncertainty bounds for the nine peril-peril correlations that are significant at 90% confidence. The global nature of these peril-peril correlations is indicated by the map on Figure 10 (*see p26*). Given the chosen confidence interval, there is a 10% probability that these results arose by chance – with 120 region-peril combinations it would be normal to expect 12 apparently significant results. The 100 repetitions of the modelling process allow the stress-testing of the robustness of these results. Where Lloyd's 10,000 Monte Carlo simulations may not have fully captured the uncertainty of a given peril-peril pair, these pairs would be expected to fluctuate between showing significant and insignificant results. Out of 100 repetitions, the number of times a significant result would be found would be less than 100. In this case, each of the significant results (*see Figure 8, p24*) is shown to remain significant in more than or equal to 97 out of 100 repetitions. This suggests that the chance of a Type I error (the incorrect rejection of a true null hypothesis, sometimes termed a "false positive") is less than 3%.

Conclusion 3: Even when there are high correlation levels between weather events, it does not necessarily follow that there will be large insurance losses.

For atmospheric hazards to cause major insurance losses, a rare major atmospheric event has to take place in combination with other circumstances conducive to such losses (e.g. a weather event affecting a major urban centre). Such circumstances are so rare that even when atmospheric conditions are conducive to a major weather event, catastrophic events do not always occur. Conversely, large losses sometimes occur in years when the correlation levels are not as high. For example, Hurricane Andrew (see case study, below), which caused one of the largest insurance losses of the 20th century, occurred in an El Niño year – a climatic feature that tends to reduce the likelihood of hurricane development.

The Corporation of Lloyd's is ultimately interested in extreme events from a capital perspective and, as noted previously, there is still a high degree of randomness in their behaviour. For a hurricane to cause major damage it doesn't just have to form, it has to survive until landfall, a process that often takes place over multiple days, and that requires wind shear to be low and pressure-steering patterns to guide storms towards land. It usually has to be of high severity and to hit a major urban centre to cause an extreme loss.

Hence it cannot be assumed that high peril index values mean there will be an extreme event in the year, nor that a low peril index means there will not be. Hurricane Andrew occurred in an El Niño year when the number of hurricanes generated in the North Atlantic, as previously noted, would tend to be lower (*see, Box 3, below, for more details*).

Lloyd's has carried out multiple sensitivity tests, particularly using different conditional event sampling distributions, including where the peril index is in 1-1 correspondence with the arising losses as an extreme sensitivity. In all tested cases, Lloyd's found no discernible impact compared to an assumption of independence, outside of sampling error.

As noted, there is clearly some level of dependency between perils since the global atmosphere and ocean is a coupled dynamical system. But the findings of both the data-driven statistical study (*see Box 2 on page 30*) and the driver-based model are that the impact of this on insurance capital modelling is expected to be negligible given the deep uncertainty surrounding the most extreme events.

As such, Lloyd's concludes that an assumption of independence for the risk groups that it assesses is currently appropriate for use in modelling its natural catastrophe risks.

BOX 3: High peril index values do not necessarily lead to extreme events

Hurricane Andrew

The study makes the point that the peril indices only indicate the background level of risk and that an extreme level of the index does not imply that an extreme insurance event will occur. Hurricane Andrew is a good illustration of this. Andrew made landfall as a Category 5 hurricane in August 1992 in Miami, Florida. Described by the Miami Herald as "the worst natural disaster ever to befall the United States", it destroyed 63,000 homes and left up to 250,000 people homeless.[128] However, during this time there was a moderate strength El Niño,[129] which often leads to lower not greater hurricane activity.

Andrew made hurricane status on 22 August and it strengthened rapidly to Category 5 over 36 hours.[130] Despite being a small storm, Andrew's landfall on 24 August caused US$25bn economic damage, $15bn of which was insured[131] ($27bn in today's terms[132]), and according to the National Hurricane Center, directly led to 26 deaths and contributed to 39 more.[133]

Yet the 1992 hurricane season as a whole was not very active, in line with the El Niño effect. One measure of season strength is known as the Accumulated Cyclone Energy (ACE) index. ACE is a measure of the energy in a hurricane over its lifetime and is defined as the sum of the squares of the wind speed at six hourly observations divided by 10,000 (to avoid the values being too large). The ACE index for an entire hurricane season is then calculated as the sum of the ACE values for all the storms in that season. The ACE index was below normal in 1992 at 76 compared to 2005 which had an ACE index of 250, the highest ever recorded.[134]

Although remembered as a Florida hurricane, Andrew also entered the Gulf of Mexico causing $500m damage to oil platforms following its re-intensification over the ocean[135] making a second

US landfall in Louisiana as a Category 3 storm. This second landfall was fortunately in a location of low population density causing just $1bn of additional economic damage.[136] Had its path been different, additional major destruction could have been caused. This is a key reason that insurance industry catastrophe models are not based solely on statistical studies of past events but also take account of the potential for losses never previously observed. Such models contain modelled hurricanes that cause losses far in excess of any past events.

Official pressure and wind speed observations of Andrew were sparse and not ideally located – the nearest being at Miami airport some five miles from the eye wall (where the strongest winds occur). This led to an early example of crowdsourcing observations where individuals were asked to report any data they had. Many such observations were received that contributed to a greater understanding of the storm.[137]

Andrew had the third lowest central pressure at landfall (922mb) in the 20th century, only surpassed by the Labor Day storm in 1935 (892mb) and Camille in 1969 (909mb).[138] Gusts of up to 150kt (172 mph) and sustained winds of 125kt (144 mph) are suspected to have occurred and a strong storm surge accompanied Andrew with peak high water marks as much as 16-23ft above sea level in some locations.[139]

Many changes to insurance processes and policies were introduced post Andrew, such as Hurricane Deductibles, greater use of reassurance, and the rise in the use of catastrophe modelling.[140] All this from an event occurring in a year when the peril index was not at an extreme value.

European Windstorms

Whilst the example of Hurricane Andrew highlights that even a low peril index value cannot rule out severe events, there remain situations where an index is a robust indicator of severe natural hazards. During the northern hemisphere winters of 2013/14[141] and 2015/16[142], the North Atlantic Oscillation was strongly positive, with the monthly North Atlantic Oscillation Index mean values peaking at +3.54 for December 2013 and +4.22 for December 2015.[143] From the analysis of peril-driver interactions, the correlation coefficient between North Atlantic Oscillation and European flood was 0.5, suggesting a tendency towards flooding in Europe in periods of positive North Atlantic Oscillation.

In these two examples, the peril index relationship is indicative of the potential for extreme rainfall (with associated flooding risk) within the European region. However, it is still a big leap from there to predict the location and severity of the event, which may only result in damaging flooding due to pre-existing conditions (e.g. already saturated soil) or persistent heavy rainfall in a specific locality (e.g. the Cumbria flooding in the UK in December 2015). Yet, here too, the converse is also true in some extreme scenarios. For example, the value for the North Atlantic Oscillation Index in December 2010 is +4.62, a month characterised by complete absence of storm and flood risk due to settled and extreme cold conditions.

Risk assessment challenges

These real world examples demonstrate that in chaotic systems there is an inherent uncertainty that cannot be fully captured in modelling processes when there is imperfect knowledge of the Earth system. The sensitivity of hurricanes or extra-tropical cyclones to small changes in "initial conditions" – those processes that initiate or inhibit their growth and formation – imparts baseline unpredictability when their prediction is based on a metric that does not perfectly describe their variability.

Modes of climate variability such as El Niño-Southern Oscillation are designed to capture large-scale mean variation in the Earth's coupled atmosphere-ocean system. In each case, they are found to drive a significant part of the mean variability of individual systems such as hurricanes or extra-tropical cyclones, but because there is a limit to their predictive capability, in practice this means assessment of climate variability has a random element when climate drivers are used for predictive purposes. Chaos does not imply randomness, but chaos combined with imperfect knowledge results in limits to the extent of Earth system predictability[144].

Conclusion 4: Weather events can still occur simultaneously even if there is no link between them.

Extreme weather events can still take place at the same time even though this study confirms for us that weather events can be modelled as independent. Indeed, Lloyd's internal model generates scenarios that show multiple massive catastrophes occurring in the same year, despite underlying assumptions of independence.

The findings of this study do not preclude extreme events from happening together, and a statistical assumption of independence does not contradict this. Such multiple events would not falsify the findings of this study unless they started to happen on a regular basis. Lloyd's own internal model, based on weather event independence, contains multiple extreme events that occur simultaneously. The internal model is used for many purposes including the calculation of statutory capital requirements. When multiple events do occur together (such as in 2011) this can be evidence they are not independent. However, it does not prove it.

Lloyd's internal model, based on an assumption of independence, contains many simulations in which multiple massive catastrophes occur in the same year – far in excess of what has been experienced in practice. These arise despite Lloyd's assumption of independence. In fact, to statistically prove two risks are not independent requires a sufficient number of instances of events occurring in close proximity. As extreme events are rare, it takes a long time to gather such information, which is why Lloyd's adopted the approach described in this study, to combine statistical information with a modelling approach grounded on a foundation of literature that outlines the greatest scientific understanding of the Earth's atmospheric and oceanic system.

Overall conclusion

The results of the modelling presented in this study demonstrate that an assumption of region-peril independence is currently appropriate for use in modelling extreme natural catastrophe risks (noting the limitations of the methodology as earlier described).

This important finding supports the broader argument that the global reinsurance industry's practice of pooling risks in multiple regions is capital efficient and that modelling appropriate region perils as independent is reasonable.

This challenges the increasingly held view among some regulators around the world that capital for local risks should be held in their own jurisdictions. Lloyd's believes this approach reduces the capital efficiency of the (re)insurance market by ignoring the diversification benefits provided by writing different risks in different locations and, in so doing, needlessly increases costs, to the ultimate detriment of policyholders. Insisting on the fragmentation of capital is not in the best interests of policyholders.

Note on the methodology

While this report finds that an assumption of independence is appropriate when modelling weather-related insurance losses, it is important to recognise the limitations of the methodology presented, which is based on the current state of climate dynamics and does not account for possible future change in the Earth's climate system. It is also based on assumptions that any interaction between weather events is captured by the methodology's driver simulations.

5 Next steps

Modellers can use external data creatively and innovatively to complement the insurance market's specialist data, and both Lloyd's and the Met Office hope that by making the model available to the public for general review (*see Appendix A for full details of the methodology*) this will serve as a starting point for further work. Lloyd's welcomes dialogue and development from any and all sectors to add to and improve the methodology. The model described here attempts to capture all the material interactions between all region perils and drivers. It is important to note that simulated data from these models is dependent upon the reliability of the data used to calculate key model parameters, bearing in mind that difference sources of information have been used to construct different drivers.

To provide a more dynamically robust model, a more complete modelling system must be considered. In this study, Lloyd's and the Met Office essentially create a climate generator based on the statistical modelling on nine key drivers. From these perils were simulated by way of a variance-covariance matrix containing correlation coefficients derived from the literature. This created a computationally inexpensive method to assess dependence, but clearly depends on the accuracy of the modelling of the key drivers. Although the interactions between drivers are implicitly accounted for by simulating each in a sequential fashion (*see Sections 2.4 and Appendix Section A2 for further details*) the accuracy is limited by the robustness of the statistical modelling methods, and implicitly by the quality of the source data. More dynamically robust results could be achieved using a fully coupled (i.e. atmosphere and ocean) global climate model, such as those used in numerical weather prediction or for global climate predictions. Once initialised with appropriate boundary conditions, these models should be dynamically self-consistent. However, numerical models introduce a new set of challenges.

Once suitable initial conditions have been chosen, the model must be run until it reaches a state of statistical equilibrium (i.e. the point at which the model "forgets" its initial conditions) which typically occurs on the order of thousands to tens-of-thousands of model years, a process known as model "spin-up". Without sufficient spin-up the model is still largely dependent on the choice of initial conditions. In cases where a model's initial parameters reside more distantly in its past, the effect these have on the state of its present-day performance decrease. Additionally, as previously discussed, climate forcings are generally not time-invariant (i.e. some global drivers are likely to be non-stationary) and a single long simulation will not be statistically robust.[145, 146] To account for this, an ensemble of model runs should be used, each of which must be sufficiently spun-up so as to ensure they are independent of each other. Each of these aspects requires substantial computing power (which is why climate models are frequently run on some of the largest supercomputers in the world), and this is before considering suitable model resolutions capable of capturing the small-scale processes necessary to replicate the driver dynamics.

Estimates of the computational resource requirement and associated costs vary significantly depending on an assessment of the appropriate time period for robust results, the model resolution and the model physics required to represent drivers of interest to suitable accuracy, and the computer architecture used. Lloyd's concludes that, currently, it would not be cost-effective to carry out a full Global Circulation Model (GCM) based analysis, particularly given the overall conclusion that an assumption of independence is valid for modelling purposes.

Lloyd's believes that additional modelling efforts would be best directed to further studies that focus on topics such as exploring the nature of extreme events within the perils themselves. GCMs and other models could be useful to explore the tails of the natural perils of interest – by producing synthetic events that have not been observed before. If this approach is explored further it will be critical to assess whether the perils are resolved in the model to a sufficient granularity in order to draw meaningful conclusions.

Appendix A: Source data & mathematical descriptions

A1. Source data

Data from the following sources are used as the basis for fitting time series models. All links are valid at time of publication.

Northern Hemisphere Drivers: Includes time series for the North Atlantic Oscillation (NAO), East Atlantic Pattern (EAP), Scandinavian Pattern (SCP) and the Pacific North American Pattern (PNA). These are identified via Rotated Principal Component Analysis,[147] which results in each index being independent of the other. These indices form the basis of generating the other 5 drivers.
Data available: http://www.cpc.ncep.noaa.gov/data/teledoc/telecontents.shtml

El Niño Southern Oscillation based on the BEST ENSO index[148] that incorporates both sea-surface temperatures as measured by Nino 3.4 and the Southern Oscillation Index (the pressure difference between Tahiti and Darwin). This provides an index that more explicitly includes atmospheric processes.
Data available: http://www.esrl.noaa.gov/psd/people/cathy.smith/best

Arctic Oscillation (AO) based on the first leading mode from EOF analysis of geopotential height anomalies at 1000 hPa[149].
Data available: http://www.cpc.ncep.noaa.gov/products/precip/CWlink/daily_ao_index/ao.shtml

Antarctic Oscillation (AAO), also known as the Southern Annular Mode (SAM), based on the index derived from EOF analysis of 500 hPa geopotential height anomalies[150, 151].
Data available: http://www.cpc.ncep.noaa.gov/products/precip/CWlink/daily_ao_index/aao/aao.shtml

North Pacific Oscillation (NPO), also known as the East Pacific – North Pacific (EP- NP) pattern.
Data available: http://www.cpc.ncep.noaa.gov/data/teledoc/ep.shtml

Dipole Mode Index (DMI), the metric of the Indian Ocean Dipole[152].
Data available: http://www.jamstec.go.jp/frsgc/research/d1/iod/iod/dipole_mode_index.html

A2. Mathematical descriptions

Driver simulations
As summarised in Section 2.3, for the nine drivers a statistical model is constructed to simulate plausible realisations. The joint distribution (model) of the nine drivers was built conditionally using the property that:

$$Pr(A, B, C) = Pr(C|A, B)Pr(B|A)Pr(A)$$

where A, B and C are random variables. Instead of thinking about a nine-dimensional joint distribution of the drivers, the methodology considers nine one-dimensional conditional ones. NAO, EA, SCP and PNA are by construction independent so the study starts by modelling those. To handle autocorrelation, ARMA time-series models were assumed. For reasons of parsimony, auto-regressive (AR) time series models were first considered, leaving the use of the more complex ARMA models only if deemed necessary. For each of NAO, SCP and PNA, an AR(1) model was sufficient:

$$Y_t = \alpha + \phi Y_{t-1} + \epsilon_t$$

where $\epsilon_t \sim N(0, \sigma^2)$ is a white noise time series, Y_t is the driver time-series, α is a model constant and $\phi, \beta, \delta, \gamma$ are model coefficients.

CCF plots indicated that EA depended upon lagged values of the other three so an AR(1) regression model was assumed:

$$Y_t = \alpha + \phi Y_{t-1} + \beta\, NAO_{t-1} + \sum_{i=1}^{6} \gamma_i\, SCP_{t-i} + \sum_{j=1}^{3} \delta_j\, PNA_{t-j} + \epsilon_t$$

Next, ENSO was modelled as an AR(4), conditional on NAO, EA, SCP and PNA as well as lags of NAO and PNA (as implied by CCF plots):

$$Y_t = \alpha + \sum_{i=1}^{4} \phi_i \, Y_{t-i} + \beta_1 \, NAO_t + \beta_2 \, EA_t + \beta_3 \, SCP_t + \beta_4 \, PNA_t + \sum_{j=1}^{7} \gamma_j \, NAO_{t-j} + \sum_{k=1}^{7} \delta_k \, PNA_{t-k} + \epsilon_t$$

AO was modelled as an AR(1) model conditional on NAO, EA, SCP, PNA and ENSO. On the basis of CCF plots, 1 month lag of NAO and PNA are also included:

$$Y_t = \alpha + \phi Y_{t-1} + \beta_1 \, \mathrm{NAO_t} + \beta_2 \, \mathrm{EA_t} + \beta_3 \, \mathrm{SCP_t} + \beta_4 \, \mathrm{PNA_t} + \beta_5 \, \mathrm{ENSO_t} + \gamma \mathrm{NAO_{t-1}} + \delta \mathrm{PNA_{t-1}} + \epsilon_t$$

AAO is represented as an AR(1) model, conditional on NAO, EA, SCP, PNA, ENSO and AO. On the basis of CCF plots, 7 month lag of NAO, 10 month lag of EA and 1 month lag of ENSO also included:

$$Y_t = \alpha + \phi Y_{t-1} + \beta_1 \, \mathrm{NAO_t} + \beta_2 \, \mathrm{EA_t} + \beta_3 \, \mathrm{SCP_t} + \beta_4 \, \mathrm{PNA_t} + \beta_5 \, \mathrm{ENSO_t} + \beta_6 \mathrm{AO_t} + \sum_{\mathrm{i-1}}^{7} \gamma_{\mathrm{i}} \mathrm{NAO_{t-i}} + \sum_{\mathrm{j=1}}^{10} \delta_{\mathrm{j}} \, \mathrm{EA_{t-j}} + \theta \, \mathrm{ENSO_{t-1}} + \epsilon_{\mathrm{t}}$$

NPO is represented as an AR(1) model, conditional on NAO, EA, SCP, PNA, ENSO, AO and AAO. On the basis of CCF plots, 1 month lag of EA and 4 month lag ENSO are also included:

$$Y_t = \alpha + \phi Y_{t-1} + \beta_1 \, \mathrm{NAO_t} + \beta_2 \, \mathrm{EA_t} + \beta_3 \, \mathrm{SCP_t} + \beta_4 \, \mathrm{PNA_t} + \beta_5 \, \mathrm{ENSO_t} + \beta_6 \mathrm{AO_t} + \beta_7 \mathrm{AAO_t} + \gamma \mathrm{EA_{t-1}} + \sum_{\mathrm{i=1}}^{4} \delta_{\mathrm{i}} \, \mathrm{ENSO_{t-i}} + \epsilon_{\mathrm{t}}$$

DMI is represented as an AR(1) model, conditional on NAO, EA, SCP, PNA, ENSO, AO, AAO and NPO. On the basis of CCF plots, 1 month lag of EA and 3 month lag NAO and 2 month lag ENSO are also included:

$$Y_t = \alpha + \phi Y_{t-1} + \beta_1 \, \mathrm{NAO_t} + \beta_2 \, \mathrm{EA_t} + \beta_3 \, \mathrm{SCP_t} + \beta_4 \, \mathrm{PNA_t} + \beta_5 \, \mathrm{ENSO_t} + \beta_6 \mathrm{AO_t} + \beta_7 \mathrm{AAO_t} + \beta_8 \, \mathrm{NPO_t} + \gamma \mathrm{EA_{t-1}} + \sum_{\mathrm{i=1}}^{3} \delta_{\mathrm{i}} \mathrm{NAO_{t-i}} + \sum_{\mathrm{j=1}}^{2} \delta_{\mathrm{j}} \, \mathrm{ENSO_{t-j}} + \epsilon_{\mathrm{t}}$$

Peril simulations

For simulating perils, information describing their dependence on the various drivers are correlation coefficients (*as described in Section 2.2*). To utilise this information, each peril and its associated drivers are assumed to follow a multivariate Normal distribution $N(\mu, \Sigma)$ whose variance-covariance matrix contains correlations coefficients, derived from literature (*see Section 2.2*) in the off-diagonals.

As an example, Australian wind depends upon ENSO and AAO with correlation -0.4 and 0.3 respectively. Assuming the peril has zero mean and unit variance, then:

$$\mu = (0, \mu_{ENSO}, \mu_{AAO}) = (0, \mu_p)$$

where μ_{ENSO} and μ_{AAO} are estimated based on simulations of perils from the models above, and the covariance matrix becomes:

$$\Sigma = \begin{pmatrix} 1 & \rho_{Awind,ENSO}\sigma_{ENSO} & \rho_{Awind,AAO}\sigma_{AAO} \\ \rho_{Awind,ENSO}\sigma_{ENSO} & \sigma^2_{ENSO} & \rho_{ENSO,AAO}\sigma_{ENSO}\sigma_{AAO} \\ \rho_{Awind,AAO}\sigma_{AAO} & \rho_{ENSO,AAO}\sigma_{ENSO}\sigma_{AAO} & \sigma^2_{AAO} \end{pmatrix}$$

where ρ indicates a correlation coefficient and σ indicates region-peril variance. Note that Σ is symmetric.

The driver-driver ρ and σ are estimated from simulated perils. Properties of the multivariant Normal then imply that the peril conditional on the drivers taking value x is Normally distributed as $N(\nu, \tau)$ where:

$$\nu = \Sigma_b \Sigma_d^{-1}(x - \mu_p)$$

$$\tau = \Sigma_a - \Sigma_b \Sigma_d^{-1} \Sigma_c$$

where ν is the conditional mean and τ is the conditional variance, and:

$$\Sigma_a = 1$$

$$\Sigma_b = \left(\rho_{peril\ ,driver1}\sigma_{driver1}, \cdots, \rho_{peril,driverN}\sigma_{driverN}\right)$$

$$\Sigma_c = {\Sigma_b}^{\top}$$

$$\Sigma_d = \begin{pmatrix} \sigma^2_{driver1} & \cdots & \rho_{driver1,driverN}\sigma_{driver1}\sigma_{driverN} \\ \vdots & \ddots & \vdots \\ \rho_{driver1,driverN}\sigma_{driver1}\sigma_{driverN} & \cdots & \sigma^2_{driverN} \end{pmatrix}$$

where Σ_b has dimensions (1 x n) and Σ_d has dimensions (n x n) and n is the number of influencing drivers.

The assumption that the perils have zero mean and unit variance has no effect on the resulting peril-peril correlations and in fact any choice will do.

The drivers are simulated on a monthly time scale, starting from January 1980, based on lagged values in 1979 such that each driver simulation starts conditional on information in 1979 (for the lagged terms in the AR models). Conditional on these driver simulations, perils are simulated after aggregating the drivers at the appropriate time scale. New drivers are simulated for each Monte-Carlo simulation.

Conditional event sampling

The following example shows how conditional event sampling can be carried out when the peril index is deemed to represent a specified quantile of the insurance loss distribution.

Let I denote the index value in a given year for a specified region-peril. Let *P* be the chosen percentile that the peril index is deemed to represent.

Translate index for chosen percentile to ensure never negative – align with a chosen quantile

$$Q_P = I + 2|\min(I)|$$

To represent the reduced sensitivity to major losses described in section 3.1 let *R* be the median relationship between the 1 in 200 insurance claims and specified quantile *P* (for example, when the translated index is at its median level the 1 in 200 claim might be 6 times larger than the 1 in 10 claim (say) – in this example *R=6* and *P=0.9*). Let *f* be a function relating the relationship between the 1 in 200 value for other levels of the index; when the index is higher than median this will be less than 1 and when the index is lower it will be greater than 1.

The 1 in 200 pseudo claim for chosen region-peril, denoted Q_{200}, is then calculated as:

$$Q_{200} = Q_P . R . f(Q_P)$$

Let Φ denote the cumulative density function of the standard normal distribution. Define $q_P = \Phi^{-1}(P)$ the quantile of the standard normal distribution with percentile *P*. In particular $q_{200} = \Phi^{-1}(0.995)$.

Let $C|I$ represent a "pseudo insurance claim" in give year conditional on peril index value I. Assume that this has a lognormal distribution.

$$C|I \sim \text{lognormal}(\mu, \sigma)$$

Where,

$$\sigma = \frac{\ln(Q_{200}) - \ln(Q_P)}{q_{200} - q_P} \text{ and } \mu = \ln(Q_P) - \sigma * q_P$$

Then $C|I$ is sampled from a lognormal distribution with quantile Q_P as required and Q_{200} as defined.

Appendix B: Peril-driver seasonality

Table 5 summarises this seasonality of peril-driver correlations. Months in red indicate the periods where the monthly driver signal exhibits correlation with the associated peril. In most cases, the driver interacts with the peril concurrently (i.e. the correlation only exists during the seasons in which the peril occurs), but in some cases there is a lagged connection, indicated by the ~ symbol in the table below[h]. In a minority of cases, the connection is more complex with both lagged and non-lagged connections. These cases are not highlighted in this table but further details can be found in the reference literature in Appendix section C.

Examples:

JFMAMJJASOND = Correlation between **DJF** (Dec to Feb) driver signal and **DJF** peril

JFMAM~~ASOND = Correlation between **MAM** (Mar to May) driver and **ASO** (Aug to Oct) peril

[h] E.g. The ~ symbol in the China-flood/AAO/SAM box represents a lagged connection between April and May AAO and July and August flooding.

Table 4 – Peril-driver seasonality

	Australia wind	Australia flood	Australia wildlife	South Africa flood	Indian Ocean tropical cyclone	Thailand/ Malaysia flood	Mexico flood	Brazil flood	China flood	European wind storm	Atlantic tropical cyclone – Gulf & Florida	Atlantic tropical cyclone – NE & Canada	NW Pacific tropical cyclone	US flood	US tornadoes	EU flood
El Niño-Southern Oscillation	JF MA MJ JA SO ND	JF MA MJ JA SO ND	JF MA MJ JA SO ND	JF MA MJ JA SO ND		JF MA MJ JA SO ND	JF MA MJ JA SO ND	JF MA MJ JA SO ND			JF MA MJ JA SO ND	JF MA MJ JA SO ND	JF MA MJ JA SO ND	JF MA MJ JA SO ND	JF MA MJ JA SO ND	JF MA MJ JA SO ND
Quasi-Biennial Oscillation																
Arctic Oscillation									JF MA MJ JA SO ND							
Antarctic Oscillation/ Southern Annular Mode	JF MA MJ JA SO ND	JF MA MJ JA SO ND		JF MA MJ JA SO ND	JF MA MJ JA SO ND	JF MA MJ JA SO ND			JF MA M~ JA SO ND							
North Atlantic Oscillation										JF MA MJ JA SO ND	JF MA MJ JA SO ND	JF MA MJ JA SO ND				JF MA MJ JA SO ND
North Pacific Oscillation									JF MA MJ JA SO ND							
Pacific North America pattern											JF MA MJ JA SO ND		JF MA ~J JA SO ND	JF MA MJ JA SO ND	JF MA MJ JA SO ND	
East Atlantic Pattern										JF MA MJ JA SO ND						
Scandinavian Pattern										JF MA MJ JA SO ND						
Indian Ocean Dipole pattern		JF MA MJ JA SO ND	JF MA MJ JA SO ND	JF MA MJ JA SO ND		JF MA M~ ~A SO ND		JF MA MJ JA SO ND	JF MA MJ JA SO ND					JF MA MJ JA SO ND		JF MA MJ JA SO ND

Strong evidence

Weak evidence

Light green = best guess where seasonality unclear from literature

~ = lagged connected between <driver> ~~ <peril>

References

[1] Climate Prediction Centre (CPC). 2008. Teleconnection Introduction [online]. Available at: http://www.cpc.ncep.noaa.gov/data/teledoc/teleintro.shtml

[2] Davey, M.K., Brookshaw, A and Ineson, S. 2014. The probability of the impact of ENSO on precipitation and near-surface temperature. Climate Risk Management, 1, p.5-24

[3] NHC NOAA. 1992. Preliminary Report: Hurricane Andrew, 16 - 28 August 1992 [online]. Available at: http://www.nhc.noaa.gov/1992andrew.html

[4] AOML NOAA. 2014. Subject: E11) How many tropical cyclones have there been each year in the Atlantic basin? What years were the greatest and fewest seen? [online]. Available at: http://www.aoml.noaa.gov/hrd/tcfaq/E11.html

[5] McChristian, L. 2012. Hurricane Andrew and insurance: the enduring impact of an historic storm [online]. Available at: http://www.iii.org/sites/default/files/paper_HurricaneAndrew_final.pdf

[6] Swiss Re. 2015. Sigma No.2/2015 [online]. Available at: http://www.actuarialpost.co.uk/downloads/cat_1/sigma2_2015_en.pdf

[7] Thorncroft, C. 2014. Variability of African Easterly Waves and their relationship with Atlantic Tropical Cyclones [online]. Available at: http://cpo.noaa.gov/sites/cpo/MAPP/Webinars/2014/04-08-14/Thorncroft.pdf

[8] Graham, S and Riebeek, H. 2006. Hurricanes: The Greatest Storms on Earth [online]. Available at: http://earthobservatory.nasa.gov/Features/Hurricanes/

[9] American Meteorological Society (AMS). 2013. Glossary: African Easterly Wave [online]. Available at: http://glossary.ametsoc.org/wiki/African_Easterly_Wave

[10] Burpee, R. W. 1974. Characteristics of the North African easterly waves during the summers of 1968 and 1969. Journal of Atmospheric Science. 31(6), pp.1556-1570.

[11] Oliver, J.E. 2005. Encyclopedia of World Climatology. Springer, Dordrecht, The Netherlands, pp. 555-556

[12] World Meteorological Organization (WMO). 2016. Significant Natural Climate Fluctuations [online]. Available at: http://www.wmo.int/pages/prog/wcp/documents/climate_system.pdf

[13] BOM. 2016. The Southern Annular Mode (SAM) [online]. Available at: http://www.bom.gov.au/climate/enso/history/ln-2010-12/SAM-what.shtml

[14] Atlantic Oceanographic and Meteorological Laboratory (AOML). 2011. Atlantic Meridional Mode [online]. Available at: http://www.aoml.noaa.gov/phod/research/tav/tcv/amm/index.php

[15] Grossmann, I. and Klotzbach, P.J. 2009. A review of North Atlantic modes of natural variability and their driving mechanisms. Journal of Geophysical Research, 114(D24), p.D24107

[16] Grossmann, I. and Klotzbach, P.J. 2009. A review of North Atlantic modes of natural variability and their driving mechanisms. Journal of Geophysical Research, 114(D24), p.D24107

[17] Foltz, G. 2011. Tropical Climate Variability: Atlantic Meridional Mode [online]. Available at: http://www.aoml.noaa.gov/phod/research/tav/tcv/amm/index.php

[18] Chiang, J. C. H. and Vimont, D. J. 2004. Analagous meridional modes of atmosphere-ocean variability in the tropical Pacific and tropical Atlantic. Journal of Climate, 17(21), pp.4143–4158.

[19] Atlantic Oceanographic and Meteorological Laboratory (AOML). 2005. Frequently asked questions about the Atlantic Multi-decadal Oscillation [online]. Available at: http://www.aoml.noaa.gov/phod/amo_faq.php

[20] Schlesinger, M.E. and Ramankutty, N. 1994. An Oscillation in the Global Climate System of Period 65-70 Years. Nature, 367, pp.723-726.

[21] Enfield, D.B., Mestas-Nunez, A. M., and Trimble, P.J 2001. The Atlantic Multidecadal Oscillation and its relationship to rainfall and river flows in the continental U.S., Geophysical Research Letters, 28 (10), pp.2077-2080.

[22] Ambaum, M. H. P., Hoskins, B. J and Stephenson, D. B. 2001. Arctic Oscillation or North Atlantic Oscillation? Journal of Climate, 14, pp.3495–3507.

[23] National Oceanic and Atmospheric Administration (NOAA). 2016. National Weather Service Glossary [online]. Available at: http://w1.weather.gov/glossary/index.php?letter=a

[24] National Snow and Ice Data Center (NSIDC). 2016. All about sea ice [online]. Available at: https://nsidc.org/cryosphere/seaice/environment/global_climate.html

[25] Vihma, T. 2014. Effects of Arctic Sea Ice Decline on Weather and Climate: a review. Surveys in Geophysics. 35(5), pp.1175-1214.

[26] Risbey, J.S., Pook, M. J., McIntosh, M. C., Wheeler, M, C. and Hendon, H. H. 2009. On the Remote Drivers of Rainfall Variability in Australia. Monthly Weather Review, 137(10), pp.3233–3253.

[27] Pook, M. J., Risbey, J. S., McIntosh, P. C., Ummenhofer, C. C., Marshall, A. G and Meyers, G. A. .2013. The Seasonal Cycle of Blocking and Associated Physical Mechanisms in the Australian Region and Relationship with Rainfall. Monthly Weather Review, 141, pp.4534–4553.

[28] Pook, M. J and Gibson, T. 1999. Atmospheric blocking and storm tracks during SOP-1 of the FROST project. Australian Meteorological Magazine, 1, (Special Edition), pp.51–60.

[29] Bureau of Meteorology (BOM). 2016. Blocking Highs [online]. Available at: http://www.bom.gov.au/climate/about/?bookmark=blockinghigh

[30] Chen, N and Majda, A. J. 2015. Predicting the cloud patterns for the boreal summer intraseasonal oscillation through a low-order stochastic model. Mathematics of Climate and Weather Forecasting. 1 (1), pp.1-20

[31] Krishnamurti, T. K and Subrahmanyam, D. 1982. The 30-50 day mode at 850 mb during MONEX. Journal of the Atmospheric Sciences, 39(9), p.2088–2095.

[32] Wang, B. 2012. Boreal Summer Intraseasonal Oscillation (BSISO) [online]. Available at: http://www.cwb.gov.tw/V7/climate/climate_info/information/lectures/14/Lecture_3_BSISO.pdf

[33] In-Sik Kang, Chang-Hoi Ho, Young-Kwon Lim, and KM Lau. 1999. Principal modes of climatological seasonal and intraseasonal variations of the Asian summer monsoon. Monthly weather review, 127(3), pp.322–340.

[34] Krishnamurthy, V and Shukla, J. 2008. Seasonal persistence and propagation of intraseasonal patterns over the Indian monsoon region. Climate Dynamics, 30(4), pp.353–369.

[35] Krishnamurthy, V and Shukla, J. 2007. Intraseasonal and seasonally persisting patterns of Indian monsoon rainfall. Journal of climate, 20(1), pp.3–20.

[36] Ding, Q and Wang, B. 2009. Predicting extreme phases of the Indian summer monsoon. Journal of Climate, 22(2), pp.346–363.

[37] Wang, B., Lee, J., Kang, I., Shukla, J., Park, C.-K. Kumar, A., Schemm, J., Cocke, S., Kug, J.-S., Luo, J.-J., Zhou, T., Wang, B., Fu, X., Yun, W.-T., Alves, O., Jin, E. K., Kinter, J., Kirtman, B., Krishnamurti, T., Lau, N. C., Lau, W., Liu, P., Pegion, P., Rosati, T., Schubert, S., Stern, W., Suarez, M and Yamagata, T. 2009. Advance and prospectus of seasonal prediction: assessment of the APCC/CliPAS 14-model ensemble retrospective seasonal prediction (1980–2004). Climate Dynamics, 33(1), pp.93–117.

[38] Lee, J-Y., Wang, B., Kang, I.-S., Shukla, J., Kumar, A., Kug, J.-S., Schemm, J. K. E., Luo, J.-J., Yamagata, T., Fu, X., Alves, O., Stern, B., Rosati, T and Park, C.-K. 2010. How are seasonal prediction skills related to models' performance on mean state and annual cycle? Climate Dynamics, 35(2-3), pp.267–283.

[39] Marine Institute. 2010. Irish Ocean climate and ecosystem status report summary 2009 [online]. Available at: http://www.marine.ie/Home/sites/default/files/MIFiles/Docs/MarineEnvironment/Summary%20of%20Irish%20Ocean%20Climate%20%26%20Ecosystem%20Status%20Report%202009.pdf

[40] Climate Prediction Centre (CPC). 2012. East Atlantic [online]. Available at: http://www.cpc.ncep.noaa.gov/data/teledoc/ea.shtml

[41] Woollings, T., Hannachi, A., and Hoskins, B. 2010. Variability of the North Atlantic eddy-driven jet stream. Quarterly Journal of the Royal Meteorological Society, 36, p.856–868.

[42] Boer, G.J., Stouffer, R.J., Dix, M., Noda, A., Senior, C.A., Raper, S., and Yap, K.S. 2001. Projections of Future Climate Change. p.529. In Houghton, J.T., Ding, Y., Griggs, D. J., Noguer, M., Linden, van der P. J., Dai, X., Maskell, K and Johnson, C.A (eds.). 2001. Climate Change 2001: The Scientific Basis. Contribution of Working Group I to the Third Assessment Report of the Intergovernmental Panel on Climate Change. Cambridge University Press, Cambridge, United Kingdom and New York, NY, USA.

[43] Bureau of Meteorology (BOM). 2016. When do El Niño and La Niña events occur? [online]. Available at: http://www.bom.gov.au/climate/enso/history/ln-2010-12/ENSO-when.shtml

[44] L'Heureux, M. 2014. What is the El Niño–Southern Oscillation (ENSO) in a nutshell? [online]. Available at: https://www.climate.gov/news-features/blogs/enso/what-el-ni%C3%B1o%E2%80%93southern-oscillation-enso-nutshell

[45] Null, J. 2016. El Niño and La Niña Years and Intensities Based on Oceanic Niño Index (ONI) [online]. Available at: http://ggweather.com/enso/oni.htm

[46] NOAA Center for Weather and Climate Prediction, National Oceanic and Atmospheric Administration (CPC NOAA). 2012.ENSO FAQ [online]. Available at: http://www.cpc.noaa.gov/products/analysis_monitoring/ensostuff/ensofaq.shtml#USimpacts

[47] Saji N.H., Goswami B.N., Vinayachandran P.N and Yamagata T. 1999. A dipole mode in the tropical Indian Ocean, Nature, 401, pp.360-363.

[48] BOM. 2012. Record-breaking La Niña events: An analysis of the La Niña life cycle and the impacts and significance of the 2010–11 and 2011–12 La Niña events in Australia [online]. Available at: http://www.bom.gov.au/climate/enso/history/La-Nina-2010-12.pdf

[49] Indian National Centre for Ocean Information Services-Global Ocean Data Assimilation System (INCOIS-GODAS). 2016. Status Of IOD [online]. Available at: http://www.incois.gov.in/portal/IOD

[50] Japanese Agency for Marine-Earth Science and Technology (JAMSTEC). 2012. Indian Ocean Dipole [online]. Available at: http://www.jamstec.go.jp/frsgc/research/d1/iod/e/iod/about_iod.html

[51] Power, S., Casey, T., Folland, C., Colman, A and Mehta, V. 1995. Inter-decadal modulation of the impact of ENSO on Australia. Climate Dynamics, 15(5), p.319–324.

[52] Salinger, M.J., Renwick, J.A and Mullan, A.B. 2001. Interdecadal Pacific Oscillation and South Pacific climate. International Journal of Climatology. 21 (14), p.1705-1721.

[53] Burroughs, W. 2003. Climate into the 21st Century. Cambridge University Press, Cambridge. p.79.

[54] Villamayor, J and Mohino, E. 2015. Robust Sahel drought due to the Interdecadal Pacific Oscillation in CMIP5 simulations. Geophysical Research Letters. 42 (4). p.1214-1222.

[55] Dong, B and Aiguo, D. 2015. The influence of the Interdecadal Pacific Oscillation on Temperature and Precipitation over the Globe Climate Dynamics, 45 (9-10), p.2667-2681.

[56] Ibid.

[57] Madden, R. A and Julian, P. R. 1971. Detection of a 40–50 Day Oscillation in the Zonal Wind in the Tropical Pacific. Journal of the Atmospheric Sciences, 28(5), p.702-708.

[58] Madden, R. A and Julian, P. R. 1972. Description of Global-Scale Circulation Cells in the Tropics with a 40–50 Day Period. Journal of the Atmospheric Sciences, 29(6), p.1109-1123.

[59] Oliver, J.E., 2005. Encyclopedia of World Climatology. Springer, Dordrecht, The Netherlands, p. 476.

[60] BOM. 2012. The Madden-Julian Oscillation [online]. Available at: http://www.bom.gov.au/climate/about/?bookmark=mjo

[61] Gottschalck, J. 2014. What is MJO, and why do we care? [online]. Available at: https://www.climate.gov/news-features/blogs/enso/what-mjo-and-why-do-we-care

[62] Kayano, M, T and Kousky, V, E. 1999. Intraseasonal (30-60 day) variability in the global tropics: principal modes and their evolution. Tellus A. 51 (3). p.373-386.

[63] Kessler, W and Kleeman, R. 2000. Rectification of the Madden-Julian Oscillation into the ENSO cycle. Journal of Climate. 13. p.3560-3575.

[64] Hurrell, J. W. 1995. Decadal trends in the North Atlantic Oscillation: Regional temperatures and precipitation. *Science*, **269**, pp.676-679.

[65] Stephenson, D.B. 2016. What is North Atlantic Oscillation (NAO)? [online]. Available at: http://www1.secam.ex.ac.uk/what-is-nao.dhtml

[66] CPC NOAA. 2012. North Atlantic Oscillation [online]. Available at: http://www.cpc.ncep.noaa.gov/data/teledoc/nao.shtml

[67] Met Office. 2015. North Atlantic Oscillation [online]. Available at: http://www.metoffice.gov.uk/learning/learn-about-the-weather/north-atlantic-oscillation

[68] CPC NOAA. 2012. North Atlantic Oscillation [online]. Available at: http://www.cpc.ncep.noaa.gov/data/teledoc/nao.shtml

[69] Walker, G.T. and Bliss, E.W. 1932. World Weather V: Memoirs of the Royal Meteorological Society. 4 (36). p.53-84.

[70] Furtado, J. C., Di Lorenzo, E., Anderson, B. T., and Schneider, N. 2012. Linkages between the North Pacific Oscillation and central tropical Pacific SSTs at low frequencies. Climate dynamics, 39(12), pp.2833-2846.

[71] Rogers, J. C. 1981. The North Pacific Oscillation. Journal of Climatology., 1, pp.39–57.

[72] Newman, M., Alexander, M. A., Ault, T. R., Cobb, K. M., Deser, C., Di Lorenzo, E., Mantua, N. J., Miller, A. J., Minobe, S., Nakamura, H., Schneider, N., Daniel J. Vimont, D. J.,Phillips, A. S., Scott, J. D and Smith, C. A. 2016. The Pacific Decadal Oscillation, Revisited. Journal of Climate [in press]. Available at: http://dx.doi.org/10.1175/JCLI-D-15-0508.1

[73] National Centers for Environmental Information (NCEI). 2015. Pacific Decadal Oscillation (PDO) [online]. Available at: https://www.ncdc.noaa.gov/teleconnections/pdo/

[74] Franzke, C., Feldstein, S.B. and Lee, S. 2011. Synoptic analysis of the Pacific-North American teleconnection pattern. Quarterly Journal of the Royal Meteorological Society, 137(655), pp.329–346.

[75] NCEI. 2015. Pacific North American (PNA) [online]. Available at: https://www.ncdc.noaa.gov/teleconnections/pna/

[76] CPC NOAA. Pacific North American (PNA) [online]. Available at: http://www.cpc.ncep.noaa.gov/data/teledoc/pna.shtml

[77] Dahlman, L. 2009. Climate Variability: Pacific - North American Teleconnection Pattern [online]. Available at: https://www.climate.gov/news-features/understanding-climate/climate-variability-pacific-north-american-teleconnection

[78] European Centre for Medium-Range Weather Forecasts (ECMWF). 2015. Why the Quasi-Biennial Oscillation matters [online]. Available at: http://www.ecmwf.int/en/about/media-centre/news/2015/why-quasi-biennial-oscillation-matters

[79] Oliver, J.E. 2005. Encyclopedia of World Climatology. Springer, Dordrecht, The Netherlands, pp.555-556.

[80] Baldwin, M.P., Gray, L.J., Dunkerton, T.J., Hamilton, K., Haynes, P.H., Randel, W.J., Holton, J.R., Alexander, M.J., Hirota, I., Horinouchi, T., Jones, D.B.A., Kinnersley, J.S., Marquardt, C., Sato, K and Takahashi, M. 2001. The Quasi-Biennial Oscillation. Reviews of Geophysics, 39(2), pp.179-229.

[81] Met Office. 2014. The recent storms and floods in the UK [online]. Available at: http://www.metoffice.gov.uk/media/pdf/n/i/Recent_Storms_Briefing_Final_07023.pdf

[82] Huesmann, A. S and Hitchman, M. H. 2001. The stratospheric quasi-biennial oscillation in the NCEP reanalyses: Climatological structures. Journal of Geophysical Research: Atmospheres. 106 (D11). p.11859-11874

[83] Rohli, R.V. and Vega, A.J. 2015. Climatology. Third edition. Jones and Bartlett. Sudbury. Massachusetts. p.131-148.

[84] Held, I. 2015. 57. Teleconnections and stationary Rossby waves [online]. Available at: https://www.gfdl.noaa.gov/blog_held/57-teleconnections-and-stationary-rossby-waves/

[85] Rhines, P.B., Rossby waves, pp.1-37. In Encyclopaedia of Atmospheric Sciences, Holton,J.R., Curry, J.A, and Pyle, J. A.(eds). 2003. Academic Press, Oxford. Available at: http://shoni2.princeton.edu/ftp/lyo/journals/Rhines-RossbyWaves-EncyOfAtmos-2002.pdf

[86] Harman, J.R., 1987. Climatology. In Boston, MA: Springer US, pp.724–727. Available at: http://dx.doi.org/10.1007/0-387-30749-4_151

[87] Coumou, D., Petoukhov, V., Rahmstorf, S., Petri, S and Schellnhuber, H. J. 2014. Quasi-resonant circulation regimes and hemispheric synchronization of extreme weather in boreal summer. Proceedings of the National Academy of Sciences of the United States, 111 (34), pp.12331-12336.

[88] CPC NOAA. 2016. Scandinavia (SCAND) [online]. Available at: http://www.cpc.ncep.noaa.gov/data/teledoc/scand.shtml

[89] Bueh, C and Nakamura, H. 2007. Scandinavian pattern and its climatic impact. Quarterly Journal of the Royal Meteorological Society. 133(629). p.2117–2131.

[90] CPC NOAA. 2016. Scandinavia (SCAND) [online]. Available at: http://www.cpc.ncep.noaa.gov/data/teledoc/scand.shtml

[91] Oliver, J.E. 2005. Encyclopedia of World Climatology. Springer, Dordrecht, The Netherlands, pp.555-556

[92] NCEI. 2015. Southern Oscillation Index (SOI) [online]. Available at: https://www.ncdc.noaa.gov/teleconnections/enso/indicators/soi/

[93] Stocker, T.F., D. Qin, G.-K. Plattner, M. Tignor, S.K. Allen, J. Boschung, A. Nauels, Y. Xia, V. Bex and P.M. Midgley (eds.). 2013. Climate Change 2013: The Physical Science Basis. Contribution of Working Group I to the Fifth Assessment Report of the Intergovernmental Panel on Climate Change. Cambridge University Press, Cambridge, United Kingdom and New York, NY, USA.

[94] Harpp, K. 2005. How do volcanoes affect world climate? [online]. Available at: http://www.scientificamerican.com/article/how-do-volcanoes-affect-w/

[95] United States Geological Survey (USGS). 2016. Volcanoes can affect the Earth's climate [online]. Available at: http://volcanoes.usgs.gov/vhp/gas_climate.html

[96] Silva, S.L. 2005. Encyclopedia of World Climatology. In Oliver, J. E.ed. Dordrecht: Springer Netherlands, pp.788–794.

[97] Silva, S.L. 2005. Encyclopedia of World Climatology. In Oliver, J. E.ed. Dordrecht: Springer Netherlands, pp.788–794.

[98] Madden, R. A and Julian, P. R. 1971. Detection of a 40–50 day oscillation in the zonal wind in the tropical pacific. Journal of the Atmospheric Sciences, 28(5), pp.702–708.

[99] Hall, J. D., Matthews, A. J and Karoly, D. J. 2001. The modulation of tropical cyclone activity in the australian region by the madden–julian oscillation. Monthly Weather Review, 129(12), pp.2970–2982.

[100] Wang, B and Xie, X, 1997. A model for the boreal summer intraseasonal oscillation. Journal of Atmospheric Science, 54(1), pp.72–86.

[101] d'Orgeville, M and Peltier, W. R. 2007. On the Pacific Decadal Oscillation and the Atlantic Multidecadal Oscillation: Might they be related? Geophysical Research Letters, 34(23), pp.doi:10.1029/2007GL031584.

[102] Schlesinger, M. E and Ramankutty, N. 1994. An oscillation in the global climate system of period 65-70 years. Nature, 367(6465), pp.723-726.

[103] Salinger, M. J., Renwick, J. A and Mullan, A. B. 2001. Interdecadal Pacific oscillation and south Pacific climate. International Journal of Climatology 21(14), pp.1705-1721.

[104] Mignot, J and Frankignoul, C. 2005. The Variability of the Atlantic Meridional Overturning Circulation, the North Atlantic Oscillation, and the El Niño–Southern Oscillation in the Bergen Climate Model. Journal of Climate, 18(13), pp.2361–2375.

[105] Stone, R. C., Hammer, G. L and Marcussen, T. 1996. Prediction of global rainfall probabilities using phases of the Southern Oscillation Index. Nature, 384, pp.252-255.

[106] Evan, A. T. 2012, Atlantic hurricane activity following two major volcanic eruptions. Journal of Geophysical Research, 117 (D6), pp.2156-2202.

[107] Iles, C.E and Hegerl, G.C. 2015. Systematic change in global patterns of streamflow following volcanic eruptions. Nature Geoscience, 8(11), pp.838–842.

[108] Vihma, T. 2014. Effects of Arctic sea ice decline on weather and climate: a review. Surveys in Geophysics, 35(5), pp.1175-1214.

[109] Barnston, A and Livezey, R. 1987. Classification, seasonality and persistence of low-frequency atmospheric circulation patterns. Monthly Weather Review, 115(6), p.1083–1126.

[110] Smith, C and Sardeshmukh, P. 2000. The effect of ENSO on the intraseasonal variance of surface temperatures in winter. International Journal of Climatology, 20(13), pp.1543–1557.

[111] Ljung, G. M. and Box, G. E. P. 1978. On a measure of lack of fit in time series models. Biometrika, 65(2), pp.297–303.

[112] Harvey, A. C.1993. Time Series Models. 2nd Edition, Harvester Wheatsheaf, NY, p.44-45.

[113] Minitab Inc. 2016. What is a Z-test? [online]. Available at: http://support.minitab.com/en-us/minitab/17/topic-library/basic-statistics-and-graphs/hypothesis-tests/tests-of-means/what-is-a-z-test/

[114] Huang, S., Chang, J., Huang, Q., & Chen, Y. 2015. Identification of abrupt changes of the relationship between rainfall and runoff in the Wei River Basin, China. Theoretical and Applied Climatology, 120(1-2), pp.299-310.

[115] Knippertz, P and Wernli, H. 2010. A Lagrangian climatology of tropical moisture exports to the Northern Hemispheric extratropics. Journal of Climate, 23(4), pp.987-1003.

[116] Toniazzo, T., and Scaife, A.A. 2006. The influence of ENSO on winter North Atlantic climate, Geophysical Research Letters, 33, L24704.

[117] López-Parages, J., Rodríguez-Fonseca, B. and Terray, L., 2015. A mechanism for the multidecadal modulation of ENSO teleconnection with Europe, Climate Dynamics, 45(3-4), pp.867-880.

[118] Hertig, E., Beck, C., Wanner, H., Jacobeit, J., 2015. A review of non-stationarities in climate variability of the last century with focus on the North Atlantic–European sector, Earth-Science Reviews, 147, pp.1-17.

[119] Duvel, J-P. 2015. Initiation and Intensification of Tropical Depressions over the Southern Indian Ocean: Influence of the MJO. Monthly Weather Review, 143(6), p.2170-2191.

[120] Ash, K. D and Matyas, C. J. 2012. The influences of ENSO and the subtropical Indian Ocean Dipole on tropical cyclone trajectories in the southwestern Indian Ocean. International Journal of Climatology 32(1), pp.41-56.

[121] Mao, R., D.-Y. Gong, J. Yang, Z.-Y. Zhang, S.-J. Kim, and H.-Z. He. 2013. Is there a linkage between the tropical cyclone activity in the southern Indian Ocean and the Antarctic Oscillation?. Journal of Geophysical Research: Atmospheres, 118(15), pp.8519-8535.

[122] Wang, B., and Chan, J. C. 2002. How strong ENSO events affect tropical storm activity over the western North Pacific. Journal of Climate, 15(13), pp.1643-1658.

[123] Sobel, A.H. and Maloney, E.D. 2000. Effect of ENSO and the MJO on Western North Pacific Tropical Cyclones, Geophysical Research Letters, 27(12), pp.1739-1742.

[124] Choi, K. S., and Moon, I. J. 2013. Relationship between the frequency of tropical cyclones in Taiwan and the Pacific/North American pattern. Dynamics of Atmospheres and Oceans, 63, pp.131-141.

[125] Allen, J. T., Tippett, M. K., and Sobel, A. H. 2015. Influence of the El Niño/Southern Oscillation on tornado and hail frequency in the United States. Nature Geoscience, 8(4), pp.278-283.

[126] Lee, S. K., Atlas, R., Enfield, D., Wang, C., and Liu, H. 2013. Is there an optimal ENSO pattern that enhances large-scale atmospheric processes conducive to tornado outbreaks in the United States? Journal of Climate, 26(5), pp.1626-1642.

[127] Cook, A. R., and Schaefer, J. T. 2008. The relation of El Niño-Southern Oscillation (ENSO) to winter tornado outbreaks. Monthly Weather Review, 136(8), pp.3121-3137.

[128] Dorschner, J. 1992. The hurricane that changed everything Miami Herald, [online] 30 Aug., p.1. Available at: http://www.nhc.noaa.gov/archive/storm_wallets/atlantic/atl1992/andrew/news/mh0828p1.gif

[129] Golden Gate Weather Services (GGWS). 2016. El Niño and La Niña Years and Intensities [online]. Available at: http://ggweather.com/enso/oni.htm

[130] NHC NOAA (National Hurricane Center, National Oceanic and Atmospheric Administration). 1992. Preliminary Report: Hurricane Andrew, 16 - 28 August 1992 [online]. Available at: http://www.nhc.noaa.gov/1992andrew.html

[131] McChristian, L. 2012. Hurricane Andrew and insurance: the enduring impact of an historic storm [online]. Available at: http://www.iii.org/sites/default/files/paper_HurricaneAndrew_final.pdf

[132] Swiss Re. 2015. Sigma No.2/2015 [online]. Available at: http://www.actuarialpost.co.uk/downloads/cat_1/sigma2_2015_en.pdf

[133] NHC NOAA. 1992. Preliminary Report: Hurricane Andrew, 16 - 28 August 1992 [online]. Available at: http://www.nhc.noaa.gov/1992andrew.html

[134] AOML NOAA. 2014. Subject: E11) How many tropical cyclones have there been each year in the Atlantic basin? What years were the greatest and fewest seen? [online]. Available at: http://www.aoml.noaa.gov/hrd/tcfaq/E11.html

[135] NHC NOAA. 1992. Preliminary Report: Hurricane Andrew, 16 - 28 August 1992 [online]. Available at: http://www.nhc.noaa.gov/1992andrew.html

[136] Ibid.

[137] Ibid.

[138] Ibid.

[139] Ibid.

[140] Ibid.

[141] Met Office. 2014. Winter 2013/14 [online]. Available at: http://www.metoffice.gov.uk/climate/uk/summaries/2014/winter

[142] Met Office. 2016. Winter 2015/16 [online]. Available at: http://www.metoffice.gov.uk/climate/uk/summaries/2016/winter

[143] Osborn, T. 2016. North Atlantic Oscillation Index data (online). Available at: https://crudata.uea.ac.uk/~timo/datapages/naoi.htm

[144] Edwards, T.L. & Challenor P.G., 2012, Risk and uncertainty in hydrometeorological hazards in J.C. Rougier, R.S.J. Sparks, and L.J. Hill (eds), 2013, Risk and Uncertainty Assessment for Natural Hazards, Cambridge, UK: Cambridge University Press.

[145] Stephenson, D.B., Collins, M., Rougier, J.C. and Chandler, R.E. 2011, Statistical problems in the probabilistic prediction of climate change. Environmetrics, 23(5), pp.364-372.

[146] Herein, M., Márfy, J., Drótos, G. and Tél, T. 2016, Probabilistic Concepts in Intermediate-Complexity Climate Models: A Snapshot Attractor Picture. 29(1), pp.259-272

[147] Barston, A. and Livezey, R. 1987. Classification, seasonality and persistence of low-frequency atmospheric circulation patterns. Monthly weather review, 115(6), pp.1083–1126.

[148] Smith, C. and Sardeshmukh, P. 2000, The effect of ENSO on the intraseasonal variance of surface temperatures in winter. International Journal of Climatology, 20(13), pp.1543–1557.

[149] Thompson, D. and Wallace, J. 1998, The arctic oscillation signature in the wintertime geopotential height and temperature fields. Geophysical Research Letters, 25(9), pp.1297–1300.

[150] Mo, K. 2000. Relationships between low-frequency variability in the southern hemisphere and sea surface temperature anomalies. Journal of Climate 13(20), pp.3599–3610.

[151] Thompson, D. and Wallace, J. 2000, Annular modes in the extratropical circulation. part I: Month-to-month variability. Journal of Climate, 13(5), pp.1000–1016.

[152] Saji, N., Goswami, B., Vinayachandran, P. and Yamagata, T. 1999, A dipole mode in the tropical Indian Ocean. Nature 401(6751), pp.360–363.